Application of Spectral Change Detection Techniques to Identify Forest Harvesting Using Landsat TM Data

Samuel D. Chambers

Thesis submitted to the Faculty of
Virginia Polytechnic Institute and State University
In partial fulfillment of the requirements for the degree

MASTER OF SCIENCE

In

GEOGRAPHY

James B. Campbell, Chair

Lawrence C. Carstensen

Randolph H. Wynne

Virginia Polytechnic and State University
Blacksburg, Virginia, 24061

July 11, 2002
Blacksburg, Virginia

Keywords: Remote Sensing, Change Detection, Landsat TM, Forest Harvesting

Application of Spectral Change Detection Techniques to Identify Forest Harvesting Using Landsat TM Data

Samuel D Chambers

(ABSTRACT)

The main objective of this study was to determine the spectral change technique best suited to detect complete forest harvests (clearcuts) in the Southern United States. In the pursuit of this objective eight existing change detection techniques were quantitatively evaluated and a hybrid method was also developed. Secondary objectives were to determine the impact of atmospheric corrections applied before the change detection, and the affect post-processing methods to eliminate small groups of misclassified pixels ("salt and pepper" effect) had on accuracy.

Landsat TM imagery of Louisa County, Virginia was acquired on anniversary dates in both 1996 and 1998 (Path 16, Row 34), clipped to the study area boundary, and registered to one another. Previous to the change detection exercise, two levels of atmospheric corrections were applied to the imagery separately to produce three data sets. The three data sets were evaluated to determine what level of pre-processing is necessary for harvest change detection. In addition, eight change detection techniques were evaluated: 1) the 345 TM band differencing, 2) 35 TM band differencing, 3) NDVI differencing, 4) principal component 1 differencing, 5) selection of a change band in a multitemporal PCA, 6) tasseled cap brightness differencing, 7) tasseled cap greenness differencing, and 8) univariate differencing using TM band 7. A hybrid method that used the results from the eight previous techniques was developed. After performing the change detection, majority filters using window sizes of 3x3 pixels, 5x5 pixels, and 7x7 pixels were applied to the change maps to determine how eliminating small groups of misclassified pixels would affect accuracies. Accuracy assessments of the binary (harvested or not harvested) change maps were used to evaluate the accuracies of the various methods described using 256 validation points collected by the Virginia Department of Forestry.

The atmospheric corrections did not seem to significantly benefit the change detection techniques, and in some cases actually degraded accuracies. Of the eight techniques applied to the original dataset, univariate differencing using TM band 7 performed the best with a 90.63% overall accuracy, while Tasseled Cap Greenness returned the worst result with an overall accuracy of 78.91%. Principal component 1 differencing and 35 differencing also performed well. The hybrid approach returned good results, but at its best returned an overall accuracy of 90.63%, matching the TM band 7 method. The majority filters using the 3x3 and 5x5 window sizes increased the accuracy in many cases, while the majority filter using the 7x7 window size degraded overall accuracy.

Acknowledgements

I would first like to thank my committee members, James B Campbell, Lawrence W Carstensen and Randolph H Wynne for their assistance and dedication over the past two years. Their instruction and mentorship has greatly enriched my life, and made my graduate experience at Virginia Tech a positive one in many ways.

I would also like to thank some of my fellow colleagues, Brent Holoviak, Jason Cash, and Awilda Velez. They have offered support in a multitude of ways. Thank you for your encouragement and motivation.

Lastly I would like to thank my parents whom have been there from the beginning, supported me through the tough times, rejoiced with me through the good times, and spent many nights praying for me to succeed. Without your dedication and help from above I could have never made it this far.

Table of Contents

List of Figures

List of Tables

1. INTRODUCTION

1.1 Importance of Monitoring Land Cover Change

Land cover change is one of the most significant disturbances to the regional environment (Vitousek, 1992; Roberts et al, 1998). The cumulative effect of land cover and land use changes can impact global climate (Lean and Warilow, 1989; Shukla et al, 1990), biogeochemical cycles (Deitweiler and Hall, 1988; Lugo and Brown, 1992), and biodiversity through habitat fragmentation (Skole and Tucker, 1993). It is vital to monitor land cover and land use change at regional and global scales. This is complex when it is considered that in many areas historic land cover data is either of poor quality, or does not exist at all (Roberts et al, 1998). Even in the United States where a large amount of historic data exists, much of the data is incompatible because of differences in spatial resolution, accuracy, periodicity, file format, classification schemes, and availability (Gildea, 2000). Simply inventorying land cover for one time is not enough. A land cover map derived from one date of imagery is essentially obsolete by the time it is created. The reason for this is that in the modern world, mankind alters land cover at a rapid pace. Furthermore, disagreement in the literature on techniques, pre-processing, post-processing, periodicity, and lack of regularly collected ground truth data all have hindered this from coming about.

Even if a repeatable, objective, and quantitatively evaluated method existed for monitoring regional change over regular periods, in itself it would not be enough. Analysis to determine the reason for the change, the long-term effects of the change, and future alternatives must be considered. Even the analysis and subsequent predictions are useless if they are not used to influence decision-makers and inform the general public.

There have been studies to monitor and inventory change that have used analysis to relate land cover change to environmental conditions. One example is the North American Landscape Characterization (NALC). The objectives of the NALC are to

develop standardized remotely sensed data sets and analysis methods in support of investigations of changes in land cover, to develop inventories of terrestrial carbon stocks, to assess carbon cycling dynamics, and to map terrestrial sources of greenhouse gas emissions (Lunetta et al, 1998). One of the primary goals of this project is monitor forestland cover, including forest distribution, land cover conversion, and forest regrowth (Lunetta et al, 1998). Since forests contain most of the world's carbon (C) stocks, to conserve significant quantities of C deforestation must be controlled and management strategies need to be implemented. In addition, the NALC has used Landsat imagery for a host of other studies, inventories, and analysis. "Some areas of application include crop acreage inventories, timber class identifications, soil association identification and mapping, range cover and forage production analysis, plant stress detection, regional land use classifications, photo-map generation, mineral and petroleum exploration, pollution monitoring, geological mapping and interpretation, areal snow extent assessments, shallow bathymetric measurements, sea ice movement monitoring, vegetation classification and mapping, surface mining operations monitoring, flood and forest fire monitoring, and beach erosion detection." (USGS, 2000)

Another study analyzed relationships between land use and land cover data and water quality trends in the Commonwealth of Virginia (Gildea, 2000). Land use and land cover is one factor that influences water quality. This study found that in general highly forested watersheds were associated with improved water quality. The study also stated that watersheds with large amounts of agricultural land and urban areas were associated with low water quality.

This study examines various change detection techniques and their effectiveness in detecting forest clearcuts. Although this study emphasizes one type of change, it is hoped that the results and conclusions in this study might be beneficial to other application of change detection.

1.2 Forestry Applications of Remote Sensing

Since the launch of Landsat 1 in 1972, the capability to monitor environmental resources and study environmental processes from space has existed (Lunetta, 1998). Over the past thirty years remotely sensed imagery has proven to be invaluable to the environmental sciences, and has been used for land cover mapping and natural resource monitoring.

The field of forestry has benefited a great deal. Remotely sensed imagery has many applications to forestry, and has been used for many uses including forest inventories (Bauer et al, 1994; Harding & Scott, 1978), forest area estimation (Wynne et al, 2000; Wayman, 2000), and forest change detection (Sader, 1995; Jano et al, 1998, Bauer et al, 1994; Colwell and Weber, 1981; Hame et. al., 1998; Hayes and Sader, 2001; Malila, 1980; Muchoney and Haack, 1994; Nelson, 1983; Singh, 1986; Green and Cosentino, 1996).

Forests are dynamic entities, and can change due to seasonal and environmental factors, as well as human activities. It is important that changes be inventoried accurately so that physical and human processes at work can be observed and understood. Traditionally foresters have relied on field inventories and aerial photography to map forest clear-cuts. Both photointerpretation and field surveys are effective, but they are both time consuming and expensive (Green and Cosentino, 1996). Medium resolution satellite imagery is an effective alternative. Coupled with aerial photography, geographic information systems, global positioning systems, and advances in computer technology, it is becoming more efficient and practical to use spaced based remote sensing data for everyday use.

1.3 Change Detection

Significant effort has gone into the development of change detection methods using remotely sensed data (Jensen et al, 1987; Jensen et al, 1991, Wheeler, 1993; Green et al, 1994; Singh 1989). Change detection can be defined as the "process of identifying differences in the state of an object or phenomenon by observing it at different times"

(Singh, 1989). The challenge in change detection is using changes in digital spectral reflectance values to determine areas of true change over time. The basic principle in change detection using remote sensing data is that changes in land cover will result in changes in reflectance values that are distinguishable from changes caused by other factors, such as differences in atmospheric conditions, environmental conditions, solar illumination, sun angle, etc (Singh, 1989).

1.3.1 Data Considerations

General steps to perform a change detection exercise are illustrated in Figure 1. After defining the nature of the change detection objective, the study area, and the frequency of the change detection, certain sensor and environmental considerations must be made.

Continuity in spectral resolution is vital when one considers that the fundamental assumption of change detection is that the difference between spectral responses of the same area will be large if land cover has changed between two dates. The sensor data used for spectral change detection should have consistent temporal, spatial, spectral, and radiometric resolutions (Jensen, 1996). The data should be acquired at the same time of the day and on or close to anniversary dates. This reduces misclassification due to differences in sun angle and seasonal differences. Spatial resolution should be the same if possible, although data with differing resolutions can be used if the data set with the finer resolution is resampled to match the data with the coarser resolution. Radiometric resolution should be held constant so the values of the both images are on the same scale.

Atmospheric conditions such as clouds, haze, and extreme humidity can introduce erroneous results to a multitemporal change detection process. Preferably data used for change detection should be clear of clouds and haze, and have similar soil moisture and vegetation phenological conditions. For change detection operations involving agriculture, forestry, or any living vegetation, phenological conditions are

extremely important. The use of anniversary dates greatly minimizes the effects of seasonal changes.

1.3.2 Image Registration

Images should be registered to one another with the best possible accuracy. Jensen (1996) recommends a root mean square error (RMSE) of 0.5 pixel or better, while Dia and Khorram (1998) suggest a RMSE of 0.2 pixels or better. Misregistration can cause false changes to appear on the change detection map, especially around class boundaries.

1.3.3 Atmospheric and Radiometric Corrections

Errors in the data set can be introduced in a variety of ways including sensor calibration errors and atmospheric effects (Jensen, 1996). Solar radiation is basically unaffected as it travels through space. However, during the transmission through the earth's atmosphere it is selectively scattered and absorbed (Jensen, 1996). Atmosphere between the terrain and the remote sensing system can attribute so much noise that the energy recorded no longer resembles the energy reflected by the terrain (Jensen, 1996). A result of atmospheric scattering is that fine detail in an image will be lost (Richards, 1995). Because both Rayleigh and Mie scattering are wavelength dependant, the atmosphere will affect the bands differently (Bernstein et al, 1983 & Richards, 1995), with the shorter wavelengths affected the most.

Radiometric corrections address variations in digital values. Causes of these variations include differing sensitivities of malfunctioning detectors, topographic effects such as shadowing and reflections, and atmospheric effects. Using published gains and offsets from the images, reflectance and radiance can be computed for an image. Acquisition dates and solar elevation must be known. Atmospheric correction involves minimizing the effects of wavelength-dependent scattering in imagery caused by haze and smoke. Many atmospheric correction methods are complex and demand *in situ* measurements and atmospheric data for the time and place the imagery was acquired. Bauer and others (1994) found that atmospheric and

General Steps Used to Conduct Digital Change Detection Using Remote Sensor Data

State the Change Detection Problem

- Define the study area
- Specify frequency of change detection (e.g. seasonal, yearly)
- Identify classes from an appropriate land cover classification system

Considerations of Significance When Performing Change Detection

- Remote Sensing System Considerations
  - Temporal Resolution
  - Spatial Resolution
  - Spectral Resolution
  - Radiometric Resolution
- Environmental Considerations
  - Atmospheric Conditions
  - Soil Moisture Conditions
  - Phenological Cycle Characteristics
  - Tidal Stage

Image Processing of Remote Sensor Data to Extract Change Information

- Acquire Appropriate Change Detection Data
  - In situ and Collateral Data
  - Remotely Sensed Data
    - Base Year (Time n)
    - Subsequent Year(s) (Time n-1 or n+1)
- Preprocess the Multiple Date Remotely Sensed Data
  - Geometric Registration
  - Radiometric Correction (or normalization)
- Select Appropriate Change Detection Algorithm
- Apply Appropriate Image Classification Logic If Necessary
  - Supervised, Unsupervised, Hybrid
- Perform Change Detection Using GIS Algorithms
  - Highlight Selected Classes Using Change Detection Matrix
  - Generate Change Map Products
  - Compute Change Statistics

Quality Assurance and Control Program

- Assess Statistical Accuracy of:
  - Individual Date Classifications
  - Change Detection Products

Distribute Results

- Digital Products
- Analog (Hardcopy) Products

Figure 1 – General steps used to conduct digital change detection using remote sensor data (Jensen, 1996).

radiometric corrections improve the accuracy of change detection results. Their change detection study attributed higher accuracy to reflectance calibration and normalization for atmospheric effects.

1.3.4 Change Detection Techniques

It is generally accepted that there are two main approaches to change detection (Lunetta, 1998; Jensen, 1996), post-classification, also referred to as map –to-map classification, and pre-classification also known as image-to-image classification.

Post-classification involves comparative analysis between two independently categorized products for different dates (Lunetta, 1998; Jensen, 1996). Two dates of imagery must first be registered to one another, and then classified separately. The two maps then must be compared on a pixel-by-pixel basis (Jensen, 1996). Originally used in the late 1970s, this method was considered the most reliable and the standard for quantitative analysis of other techniques (Weismiller et al, 1977). An advantage of this method is that data normalization between the two images is not required because they are classified separately (Singh, 1989). A disadvantage of this method is that the errors on both of the categorized images will be present and have a multiplicative effect on the change detection product (Stow et al, 1980; Lunetta, 1998; Rutchey & Velcheck, 1994). This causes a large number of erroneous change indications since an error on either image gives a false indication of change (Singh, 1989).

The pre-classification approach involves the simultaneous analysis of multitemporal data (Singh, 1989). A wide variety of pre-classification techniques have been developed, including composite analysis, image differencing, principal components analysis, change vector analysis, and spectral mixture analysis (Lunetta, 1998). The following paragraphs discuss specific pre-classification techniques in more detail.

Multi-date composite analysis involves placing multiple dates of imagery into the same dataset and analyzing the composite dataset. Muchoney and Haack (1994) took

two images of the same area but different dates, and merged the two images. Once the bands were "stacked", they performed a maximum likelihood classification. Their study showed that using images with similar conditions but different dates, change areas show major differences statistically when classification techniques are applied to the data. This technique is sometimes called direct multi-date classification. A disadvantage to this technique is that the combined interpretation of land cover in addition to change classes is complex. Walsh (1979) used this technique to classify Landsat MSS data sets acquired over different seasons in the same year to improve the accuracy of land use and land cover classes.

Another multi-date technique, selective principal components analysis (SPCA), entails performing a PCA on the composite dataset, and then identifying and thresholding the change component. Monitoring land cover change using PCA was first reported by Byrne and others (1980). Experiments have demonstrated that if the change occurs only on a small percentage of the study area, the first and second principal components tend to represent the unchanged land cover, while the third and later principal components contain the change information (Byrne et al, 1980; Richards, 1984; Lunetta, 1998). Jiaju (1988) demonstrated the ability of PCA to separate crop types.

Image differencing is performed by calculating a subtraction product for two digital complementary data sets, then applying a threshold to distinguish significant spectral differences as areas of change (Lunetta, 1998; Yuan et al, 1998). "The subtraction results in positive and negative values in areas of change, and zero values in areas of no change in a new change image (Jensen, 1996)". It is common to transform the numbers into positive values by adding a constant value such as 128 to the data. The change image usually yields a digital number distribution Gaussian in nature, where the pixels of no change are distributed around the mean and the change pixels are found in the tails of the distribution (Price et al, 1992; Jensen, 1996). In its simplest form, image differencing may be univariate, which means that a single band from each image is chosen, then one is subtracting from the other. Data transformation

techniques to reduce data dimensionality may be applied prior to subtraction (Lunetta, 1998). These include band ratioing, vegetation indices, PCA, and tasseled cap transformation. A disadvantage to the differencing method is that it only identifies areas that have changed but provides no information on the nature of the change (Jensen, 1996).

Change vector analysis gives not only a change map, but a change direction product as well. The length of the vector indicates the magnitude of change and the direction indicates the nature of the change (Lanbin & Strahler, 1994; Jensen, 1996; Lunetta, 1998). Change vector analysis has been used for forest change detection in northern Idaho (Malila, 1980).

Image ratioing takes two registered images from different dates and performs division on them using certain bands. In areas of change the ratio value would be significantly greater than 1 or less than 1 depending on the nature of the change. Areas of no change should have a value close to 1. Image ratioing was has been used to detect change detection in land cover (Stow et. al., 1990) and for forest canopy change (Green and Cosentino, 1996).

A multitude of additional methods have been discussed in the literature, too numerous to list. The methods mentioned above are the most common in the literature.

1.3.5 Thresholding

An important step in most pre-classification change detection operations is deciding where to place the threshold boundary between change and no-change. The distribution of pixels in a change map is usually normal, and there is not an obvious break to place a threshold (Figure 2). A constant of 128 is usually added to the change image so that values are positive. This shifts the mean from around 0 to a value close to 128. Areas of no change are usually grouped around the mean value while change areas are found on the tails of the histogram. One method for delineating thresholds involves selecting a standard deviation from the mean (Jensen,

1996). Another method, visually inspecting the distribution (histogram) and to placing a threshold along the tails, is also common. Most analysts prefer to experiment empirically, placing the threshold at various locations in the tails of the distribution until the amount of change seems realistic, either by visual inspection, in situ knowledge of the study area, or by an error matrix if validation data exists (Jensen, 1996). Thus the selection of a threshold can be subjective in nature (Jensen, 1996; Singh, 1989). Wynne and Scrivani (2000) developed a objective and repeatable method using a C++ program that takes known points as inputs then sets a threshold so that the overall accuracy of a binary harvest/no harvest image would meet some pre-specified criterion. Applying a threshold to the image generated by the change detection algorithm produces a thematic change map is created.

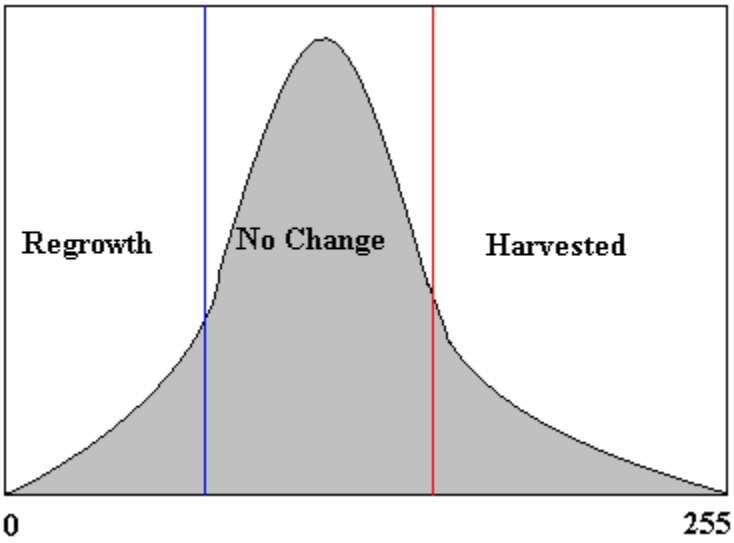

Figure 2 – Histogram curve showing thresholds used to extract areas of change.

1.3.6 Accuracy Assessment

One of the most important steps of a change detection exercise is the accuracy assessment of the change map. Many studies of change detection, especially in the early literature, failed to perform qualitative assessments of the change products using validation points. The appearance of the map or personal knowledge was used in some cases.

According to Campbell (1996) “accuracy should be evaluated through a well-defined effort to assess the map in a manner that permits quantitative measure of accuracy and comparisons with alternative images of the same area”. Although there exists a vast quantity of historic remotely sensed data, the existence of validation points collected in the field at regularly spaced intervals is rare, and in most cases does not exist. Many times the points for past locations must be assembled using ancillary data such as large scale aerial photography, land cover maps, or other historic data. Planned land cover change detection exercises may allow validation points to be collected in the field around the data acquisition date, so errors will be minimized. Location of the samples should be considered, and should be adequately representative of the no change and change classes and distributed evenly throughout the entire study area.

Most change detection studies use a contingency (error) matrix similar to the one used in image classification exercises. Overall accuracy, producers accuracy, users accuracy, errors of omission, errors of commission, Kappa and Kappa variance all can be derived from the error matrix. In addition contingency matrices can be compared to return Z-scores.

2. OBJECTIVES

Although a variety of techniques are available for change detection, little information exists to permit the identification of the best method for forest harvest detection. Many studies that evaluate the different methods contradict one another, and very few of the studies have ancillary data such as validation points and masks to verify the results.

The main objective of this study was to determine the spectral change technique best suited to detect complete forest harvests (clearcuts) in the Southern United States through the process of comparing eight techniques and evaluating them in a quantitative manner. They were the 1) TM band 345 differencing, 2) TM bands 35 differencing, 3) NDVI differencing, 4) first principal component differencing, 5) selection of a change band in a multitemporal PCA, 6) tasseled cap brightness differencing, 7) tasseled cap greenness differencing, and 8) a univariate differencing technique using TM band 7. Using information from the previous methods a hybrid method was developed to determine if higher accuracies could be achieved using by using a combination of methods.

Secondary objectives were to determine if radiometric and atmospheric corrections are necessary steps before the change detection, and if post-processing methods to eliminate small groups of misclassified pixels ("salt and pepper" effect) significantly affect accuracy.

3. PURPOSE

The Commonwealth of Virginia is comprised of an estimated 15.4 million acres of forestland, with 8.5 million acres available for timber production (Scrivani, 2000). The cost of aerial photography or ground surveys would be quite expensive compared to the use of medium resolution imagery to cover such a large region. Forest harvests need to be identified using a repeatable, objective, and accurate method. The ability to quickly and efficiently perform annual change assessments is a great tool that should be available to foresters in Virginia.

Another potential application for harvest identification using change detection techniques is verifying riparian buffer zones for environmental and tax purposes. The following is an excerpt from an article about the Riparian Forest Buffer Tax Credit in VDOF Virginia Forest Landowner Update (VDOF, 2001):

> "The 2000 General Assembly enacted the Riparian Buffer Tax Credit to provide a non-refundable tax credit to individuals who own land on which timber is harvested, which abuts a waterway, and who forebear timber harvesting on certain portions of the land for 15 consecutive years"

If historical imagery exists and annual harvest change detection is performed, it would be a simple task (assuming resolution is adequate) to determine where land met the requirements for the Riparian Buffer Tax Credit. At this time, no method exists to verify these tax credits. Determination of the most effective spectral change detection technique, including the levels of pre and post-processing required, would allow an efficient and standard method to detect clearcuts allowing the Commonwealth of Virginia to verify that tax credits are justified.

4. LITERATURE REVIEW

Change detection techniques using medium resolution remotely sensed satellite imagery has been applied to such diverse areas as urban, coastal, desert, glacial, and shallow reef environments. Change detection studies to monitor general land cover, forestry, agricultural, and urban changes are common. Events causing changes from natural hazards including fire, hurricanes, landslides, earthquakes as well as man made catastrophes (Chernobyl, Kuwait) have been monitored. Using airborne mounted laser sensors, change detection of buildings and man made structures has recently been studied. The Canadian military even published a study using medium resolution imagery to detect troop movements, specifically the Soviet withdrawal from Afghanistan (Banner, 1991).

Change detection involves not only detection, but also specification of location and extent of that change, and sometimes the identification of the actual change (from/to). Interpretation of the actual cause of the change is normally left to the analyst. Deers (1995) concluded that there is no optimal change detection technique, that the choice is application dependant. He goes on to state that few comparative studies of change detection techniques have been reported, and the majority did not support their conclusions by quantitative analysis. Furthermore, he states that the reason many studies of change detection make no attempt at an accuracy assessment is due to a lack of reliable temporal ground reference data. Even the question of which is best for any particular application is not resolved, and unless adequate, quantitative accuracy assessment is undertaken new work will not resolve the technique is best for various applications. Although much of the early literature did not quantitatively evaluate change detection techniques, most of the recent literature reports quantitative results. However, even when quantitatively evaluated, the results and conclusions vary and do not point to one best method.

Weismiller et al (1977) compared image differencing and post-classification techniques for a costal zone change detection study, but no ground reference accuracy assessment was done. Univariate image differencing, post-classification comparison, and principal component differencing were compared for urban change detection, but only qualitative analysis was done (Toll et. al., 1980). Post-classification comparison, change vector analysis, and visual estimates were used for forest change detection (Colwell and Weber, 1981), but no ground reference accuracy assessment was performed. Image rationing and post-classification comparison were qualitatively compared for environmental change detection (Howarth and Wickware, 1981). Sloggett and others (1994) examined several change detection techniques for use in updating maps, and although they presented no quantitative assessment, they offered comments on the advantages and disadvantages of each. Nelson (1983) found vegetation index differencing to be superior to image differencing and rationing. Banner and Lynham (1981) found it to be less accurate than multi-date classification.

Singh (1986 & 1989) did some extensive work on the objective evaluation of automated methods for forest change detection where he compared univariate image differencing, image ratioing, NDVI differencing, image regression, PCA, post-classification comparison and multi-date classification. Many local spatial processing techniques (image smoothing, background subtraction, edge enhancement) were also investigated. He also tested threshold levels. His conclusions were that the regression method using Landsat MSS band 2 produced the best accuracy, while the post-classification method returned the lowest accuracy. Image ratioing and image differencing both performed well while local spatial processing techniques did not improve accuracies.

Fung and LeDrew (1988) and Jiaju (1988) found that SPCA performed better than image differencing and image ratioing. Stow and others (1990) reported that image ratioing produced higher accuracies than SPCA. A change detection study of forest defoliation due to the gypsy moth in Virginia reported that image differencing was better than selective PCA using the third band, but both were better than post-

classification comparison or multi-date classification (Muchoney and Haack, 1994). Martin (1989) concluded that post-classification comparison gave better results than multi-date classification or PCA.

Macleod and Congalton (1998) compared post classification, image differencing, and principal components techniques to detect change in eelgrass beds. They found that image differencing was significantly better for detecting change in submerged aquatic vegetation (SAV). Lyon and others (1998) compared vegetation index differencing using seven different indices to detect land cover changes in Chiapas, Mexico. They reported that NDVI was the least affected by topographic factors and the only technique with a normal distribution. In a study to detect vegetation changes associated with extensive flooding, NDVI image differencing outperformed Selective PCA, Selective PCA of NDVI images, spectral-temporal change classification, and temporal change classification based on NDVI (Michener & Houhoulis, 1997). Hayes and Sader (2001) compared NDVI image differencing, SPCA, and RGB-NDVI and found RGB-NDVI to be superior.

Green and others (1994) compared univariate image differencing techniques for Landsat TM, and found band 7 to be exceptional for clearcut identification if imagery was acquired on anniversary dates. Univariate image subtraction was considered desirable due to its simplicity and easy implementation in a commercial environment. Another study (Green and Cosentino, 1996) found that using image differencing of ratios of the near and mid infrared bands provided the highest accuracy in measuring crown cover change. TM7/TM4 and TM5/TM4 outperformed TM7/TM3, TM5/TM3, TM7 differencing, NDVI differencing and TM5 differencing. However the study stated that using TM5 or TM7 might be simpler and more efficient due to the fact that ratio images created more pixel noise than univariate differencing methods.

A comparison of techniques to detect land cover changes in Campeche, Mexico using Landsat MSS data found that post classification was more accurate than image

differencing, NDVI differencing, SPCA, direct multidate unsupervised classification, and a post classification / image enhancement combination (Mas 1999). Ridd and Liu (1998) compared image differencing, image regression, tasseled cap transformation, and Chi square transformation in an urban environment. They reported that the regression of TM band 3 returned the most accurate results, while differencing and regression using TM band 4 was the least accurate. Hame and others (1998) created an unsupervised method for change detection that they used to reliably detect clear-cuts in southern Finnish Boreal forest using TM data. They did not compare the results to other methods.

These comparative studies do not agree, even those that support conclusions with quantitative accuracy assessment. It is not clear from the literature that a universally optimal technique exists. Deers (1995) suggested that the choice of techniques might be dependant not only on the application but on specific data sets as well.

In addition, there is conflict in the literature in regards to atmospheric and radiometric corrections of the imagery before change detection is performed. For example, a change detection study in Minnesota used to classify canopy increase, decrease, and no change over a six-year time period attributed higher accuracy to atmospheric corrections (Bauer et al, 1994). Song and others (2001) stated that the decision to atmospherically correct imagery, and what method to use depends on the information desired and the methods used to extract information from the imagery.

5. METHODOLOGY

5.1 Study Area

Louisa County is located in the Piedmont region of the Commonwealth of Virginia and was chosen due to harvesting activity and the availability of data including Landsat TM imagery for 1994 and 1998, a forest/non-forest mask, and validation points for this time period. The location of Louisa County, VA is shown in Figure 3. Louisa County is highlighted in red.

Figure 3 – Study area location.

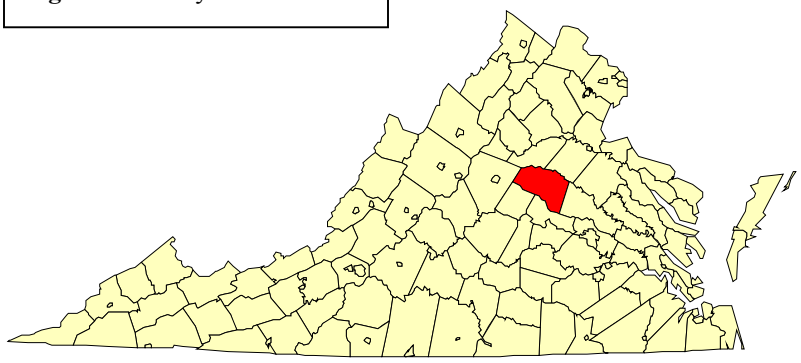

> "The county is approximately 317,800 acres and includes 228,500 acres of forested land which is predominately privately owned. Hardwoods, mostly oak-hickory type, makes up roughly 70% of the forests (163,000 acres), oak-pine mixed comprises 7% of the forests and pine types make up 21% of the total. Economically important species include the loblolly, shortleaf, Virginia pine, white oak, northern red oak, southern red oak, yellow poplar, and sweet gum. Surrounding metropolitan areas include Charlottesville, Richmond, and Fredericksburg." (USDA, 1992)

In 1996 Louisa's forest products contributed over $150 million to the local and regional economy. This indicates that there was a significant amount of harvesting between the two dates of imagery selected for this study.

5.2 Reference Data

The Virginia Department of Forestry (VDOF) collected reference data that was used to perform accuracy assessments. Two hundred and fifty six points, labeled either harvested or non-harvested were collected in Louisa County, Virginia. The methodology used to collect the two hundred and fifty six points is explained in detail in the following paragraph.

Strata were created, as follows: First, the 1994 and 1998 images without any radiometric corrections was used with seven spectral change detection techniques. The techniques were NDVI, PC1, TCB, TCG, SPCA, 345, and 35. Subsequent to automatic, objective thresholding designed to maximize producer's accuracy followed by application of a non-forest mask, results from each of these techniques were run through the Clump and Eliminate routines in Erdas Imagine to ensure that all identified harvest areas were at least 10 acres in size. An eighth scene in which harvests were identified using spectral mixture analysis techniques was treated in the same fashion. The eight resulting images were stacked. The nine strata that resulted from this stacking were based on the number of times a single ground cell was determined to be a forest harvest, ranging from 0 to 8. In each of the strata for which one or more techniques showed a "harvest" approximately 20 random samples were drawn, which were visited in the field using GPS navigation and existing FIA landowner agreements or examined on aerial color videography acquired for the purpose of this study. 110 samples were similarly drawn from the portions of the county where no forest harvests were identified. (Wynne, 2002)

Many of the points collected were sampled close to boundaries between harvested and non-harvested areas. Samples were heavily concentrated in harvested locations. Out of the 256 points 146 were sampled in harvested areas, although only a small percentage of the area was harvested. The spatial distribution of the validation points is displayed in Figure 4. Harvested (clearcuts) survey locations are shown as red points, while non-harvested survey locations are shown in as blue points.

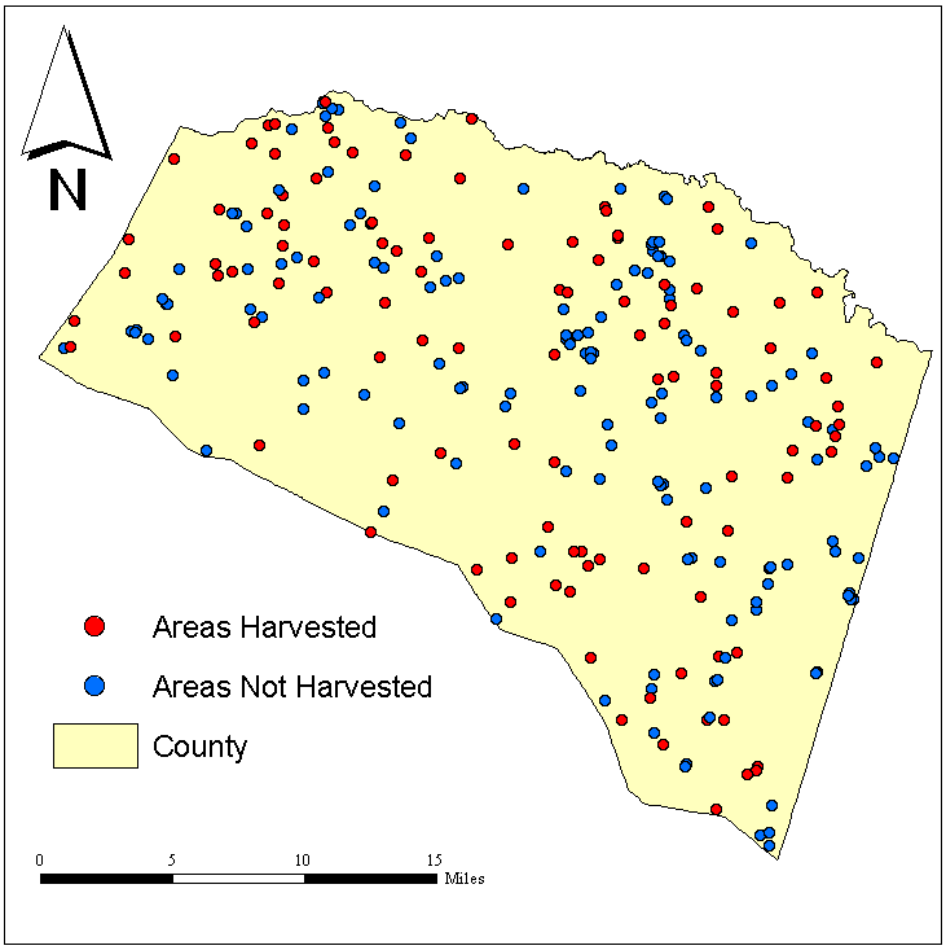

Figure 4 – Spatial distribution of 256 validation points in Louisa County, VA.

5.3 Non-Forest Mask

A non-forest mask produced by the VDOF was used to eliminate non-forested areas during the change detection study. The mask was created using heads-up digitizing over digital panchromatic orthophotographs of the county with a ground resolution of 2 feet using then-current FIA definitions of forest and non-forest (Wynne, 2002). The mask was created using 1994 orthophotography and eliminated areas not considered forested, including agricultural land, urban, and suburban areas. Shown in Figure 5, the red areas are classified non-forest, and were masked out of the study area. 26.6% of the study area (84,147.1 acres) was considered non-forest. It is important to eliminate suburban and urban areas so trees that are cleared on that property do not show up as forest harvest.

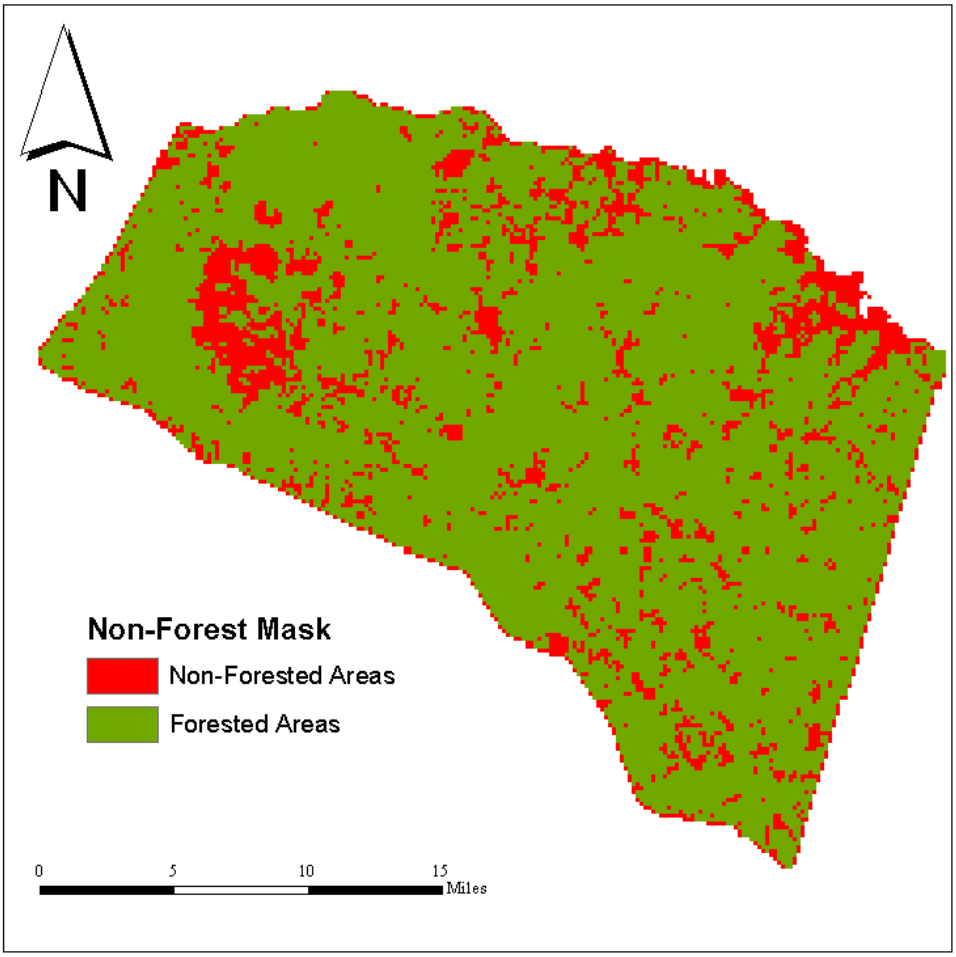

Figure 5 – Non-forest mask, Louisa County, VA.

5.4 Imagery

Landsat TM data is ideal for statewide forest harvest detection due to its spatial and temporal resolution and synoptic view. Imagery for this study was collected using the Landsat 5 satellite, which has a swath of 185 kilometers and a temporal resolution of 16 days. It observes each scene at approximately 10:00am local time. Landsat TM collects imagery in seven spectral bands with a 30-meter spatial resolution in six bands and 120m resolution in its thermal band (Table 1). In this case Landsat TM band 6 (Thermal IR) was not used, so all analysis was performed using two 6-band images. Both images had a radiometric resolution of 8-bits, therefore pixel values ranged from 0 to 255.

Band Number	Data Recorded	Spectral Resolution (micrometers)	Spatial Resolution (meters)
Band 1	Blue	0.45 – 0.52	30
Band 2	Green	0.52 – 0.60`	30
Band 3	Red	0.63 – 0.69	30
Band 4	Near IR	0.76 – 0.90	30
Band 5	Mid IR	1.55 – 1.75	30
Band 6	Thermal IR	10.40 – 12.50	120
Band 7	Mid IR	2.08 – 2.35	30

Table 1 – Information about Landsat TM data.

The imagery for this project consists of two leaf-off scenes from path 16 row 34, acquired in 1994 and again in 1998 (Table 2). Both images were acquired in late fall. Data was collected near anniversary dates to reduce scene-to-scene variation due to factors such as sun angle, sun azimuth, atmospheric conditions, vegetation phenology, and soil moisture. Each image was rectified to the VA State Plane Coordinate System South using a high-resolution roads layer. The root mean square error for both rectifications was below 0.2 pixels, as Dai and Khorram (1998) has shown that a registration accuracy of less than 0.2 pixels is needed to achieve a change detection error of less than 10%. The images were clipped to the boundary of Louisa County. The images were both cloud free in the study area, although slight haze could be observed in some areas.

Year	Month	Day	Sun Elevation	Sun Azimuth
1994	Oct	1	41.65	141.12
1998	Sept	26	45.86	146.4

Table 2 – Information on the Landsat TM imagery used in the study.

5.5 Atmospheric Corrections

The accuracy of change detection methods can be affected by a number of factors, including atmospheric influences. Corrections attempt to eliminate distortions due to differences in the atmospheric conditions on the dates that imagery was acquired, and to normalize the two dates of imagery. A concern is whether corrections actually introduce errors into the process. Even if the corrections do increase the accuracy of

the change detection operations, there is still the question of whether the additional time and effort needed to correct the images is worth the gains in accuracy produced.

This study attempts to determine if the corrections increase or decrease the overall change detection accuracies of forest harvest detection, and if the results are significant enough to consider this a necessary procedure. Two levels of corrections were applied, one fairly simple and the other a complex algorithm. The three image sets used in the study included the following:

1. Raw imagery (no corrections applied),
2. imagery converted to reflectance,
3. and converted to reflectance with an atmospheric correction applied.

For the second data set the original images were converted to exoatmospheric reflectance using published post-launch gains and offsets using ENVI image processing software. Reflectance can be defined as the fraction of the total radiant flux incident upon a surface that is reflected (Raabe & Stumpf, 1997). Reflection varies accordingly to the wavelength distribution of the incident radiation (Raabe & Stumpf, 1997). The reflectivity of the Earth's surface varies according to the positional relationship between the Earth and the Sun; the elliptical nature of the Earth's orbit causes the amount of solar irradiance to vary (Varlyguin et al, 2001). Solar irradiance on the earth is dependant upon the solar elevation, which varies according to the time of year and the location on the Earth. Conversion to exoatmospheric reflectance was used to adjust the reflectance values to consider this variance, and to normalize the imagery. The digital counts in the image are transformed to reflectance (ρ_ρ) using the calibration that comes with the files and the equations and constants of Price (1987), and Markham and Barker (1985).

$$\rho_\rho = \frac{\pi * L_\lambda * d^2}{ESUN_\lambda * \cos(\theta s)}$$

Where;
L_λ – is the spectral radiance at the sensors aperture,
d – is the normalized Earth-Sun distance,
θ_s – is the solar zenith angle at the image center, and
$ESUN_\lambda$ – is the band dependent mean solar exoatmospheric irradiance.

Using published gains and offsets from the images, the reflectance was computed for the 1994 and 1998 images using ENVI image processing software. The date of acquisition and solar elevation of the image had to be manually entered, and the program converted the image and created a new image. The new image was then rescaled to 8 bits to keep radiometric resolution constant. An example of the effect the conversion to reflectance had on the image is shown in Figure 6.

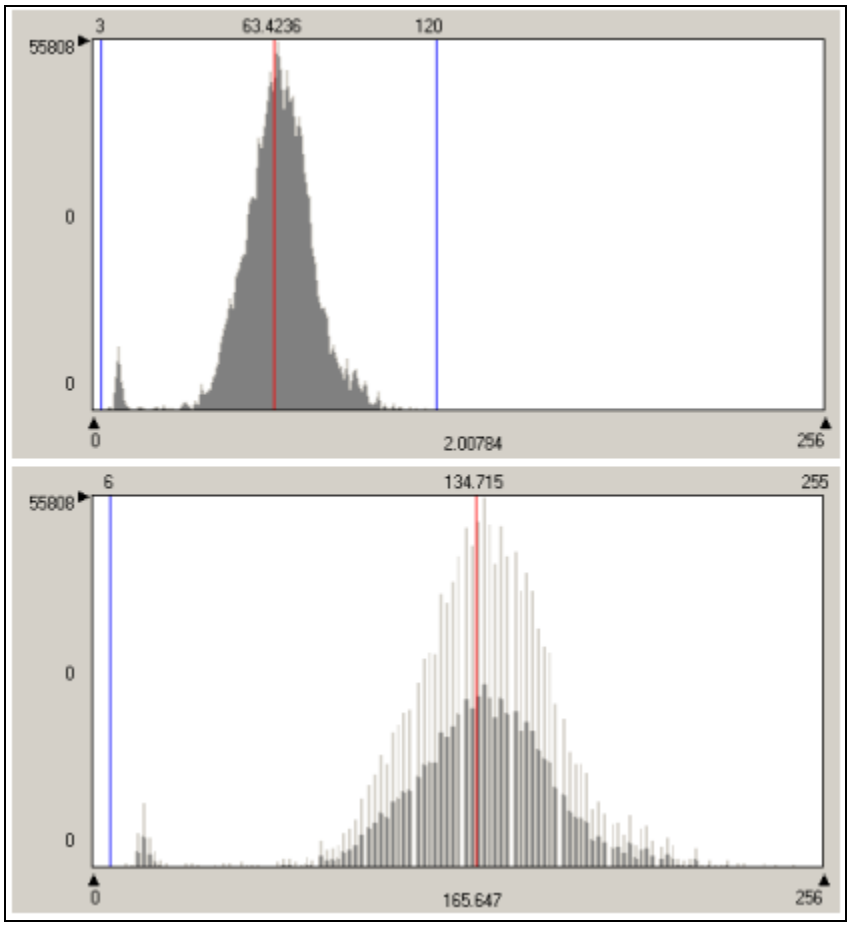

Figure 6 –The band 4 histogram from the 1998 image before (above) and after (below) conversion to reflectance.

The third data set was converted to exoatmospheric reflectance and atmospherically corrected by Science Applications International Corporation (SAIC). The atmospheric correction algorithm uses a multispectral version of ATREM (Atmospheric Removal) with the Malkmus band model for transmission, and 6S for the scattering and reflectance calculations (Wynne and Scrivani, 2000). The 6S algorithm takes into account atmospheric effects such as gaseous absorption by water vapor, carbon dioxide, oxygen, ozone and scattering by molecules and aerosols.

The three image pairs were used for seven change detection algorithms. The change detection algorithms used are listed in Table 3 along with abbreviations and formulas. The change maps generated by the change detection algorithms were assessed for accuracy to determine if higher levels of preprocessing lead to higher overall accuracies.

5.6 Change Detection Techniques

Change detection operations are ideal to identify and monitor changes caused by forest harvesting. Various change detection techniques are explored in literature, but little information exists to identify the optimal technique to use for this application. This study attempts to help fill that void, comparing techniques in a quantitative manner.

The techniques used in this study are all pre-classification, or image-to-image techniques. Eight change detection techniques, listed in Table 3 along with their abbreviations and formulas, were evaluated in this study. Although each of the eight techniques have been previously documented in earlier literature, they had to be designed and implemented using the model builder function in Erdas Imagine image processing software. Figure 7 shows an example of a model set up in Erdas Imagine. This model was designed to implement the NDVI differencing change detection technique. Prior to running the model, NDVI is performed on each image (1994 and 1998), and the resulting images are used as the inputs. Other input images include a "zero image" that eliminates the background of the image, and a non-forest mask.

Method	Abbreviation	Formula
Image Differencing using bands 3 and 5	35	(3b – 3a) - (5b – 5a)
Image Differencing using bands 3, 4 and 5	345	(3b – 3a) -(4b – 4a) + (5b – 5a)
Image Differencing using PC band 1	PC1	(PC1b - PC2a)
Selection of "change" band in a multitemporal PCA	SPCA	
Image differencing using tasseled cap "brightness"	TCB	(TCBb – TCBa)
Image differencing using tasseled cap "greenness"	TCG	(TCGb- - TCGa)
Image differencing of NDVI bands	NDVI	(NDVIb – NDVIa)
Image differencing of TM band 7 (Mid Infrared)	TM7	(TM7b – TM7a)

Table 3 – Change detection methods used in the study. In the formula column, a = the 1994 image and b = the 1998 image.

The circles in the model represent the operations. The first operation in this method is the algorithm, in this case subtracting one image from the other. The subsequent operations include thresholding, setting the background to zero, and application of the non-forest mask. Thresholds were placed at various locations in the tails of the distribution until overall accuracy was maximized. The model created two output images, one image with the pixels reclassified according to the algorithm, and another thematic change map. The change maps were coded with two values. A value of 1 was assigned to non-harvested areas and a value of 2 for harvested areas.

Using the two image sets, the swipe function in Erdas Imagine which essentially allows you to overlay one image on the other and then “peel” the top layer, was used to visually locate harvested and areas. A polygon was digitized around ten different harvested areas, and was set on top of the change images created by the different change detection techniques. The pixel values inside the harvested polygons were examined and compared to non-harvested values found immediately outside the polygons. By this method an initial threshold was estimated, applied to the change image, and evaluated quantitatively. In an iterative fashion values above and below the initial threshold were applied to the change image and evaluated quantitatively, until overall accuracy was maximized. Producer’s and User’s accuracy for each class was not considered in the threshold selection process.

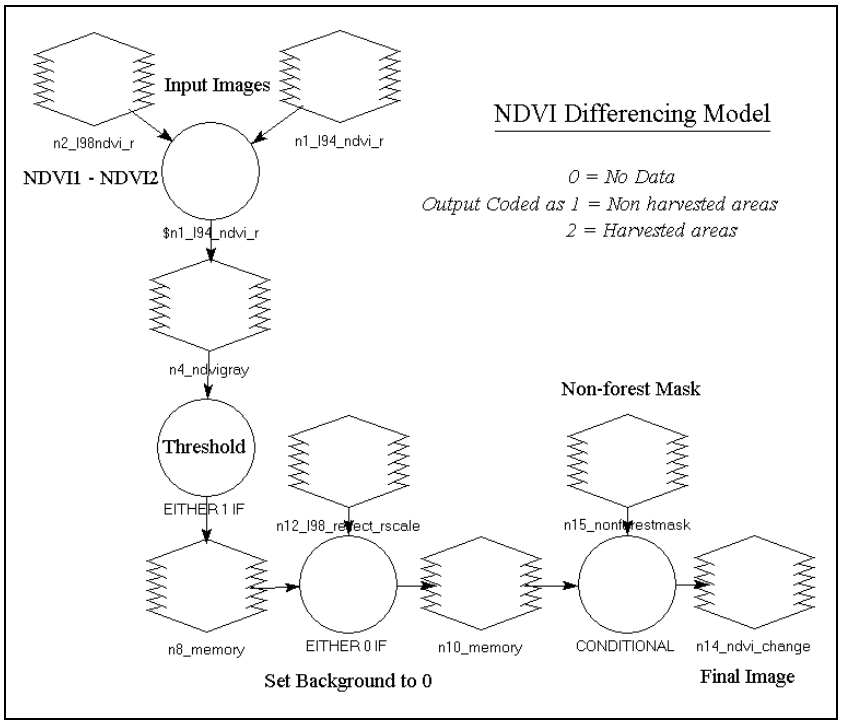

Figure 7 –Example of a change detection model (NDVI differencing).

Figure 8 is a visual example of the change detection processes using the SPCA method. The same area is circled on each image. Figure 8a shows the area in the 1994 image and Figure 8b the same area in the 1998 image. Since both input images are shown in the 432-band combination, reds represent healthy vegetation and blues represent bare soil and paved surfaces. Areas that changed from red in 1994 to blue in 1998 are areas that have been clearcut. In the SPCA change band (Figure 8c), forest regrowth shows up as black, clearcuts show up as white, and gray areas experienced little to no change. The final image (Figure 8d) is the thematic image after thresholding was applied. Yellow areas are classified non-harvest while green areas are classified harvest. In the following paragraphs the eight techniques used will be discussed in more detail.

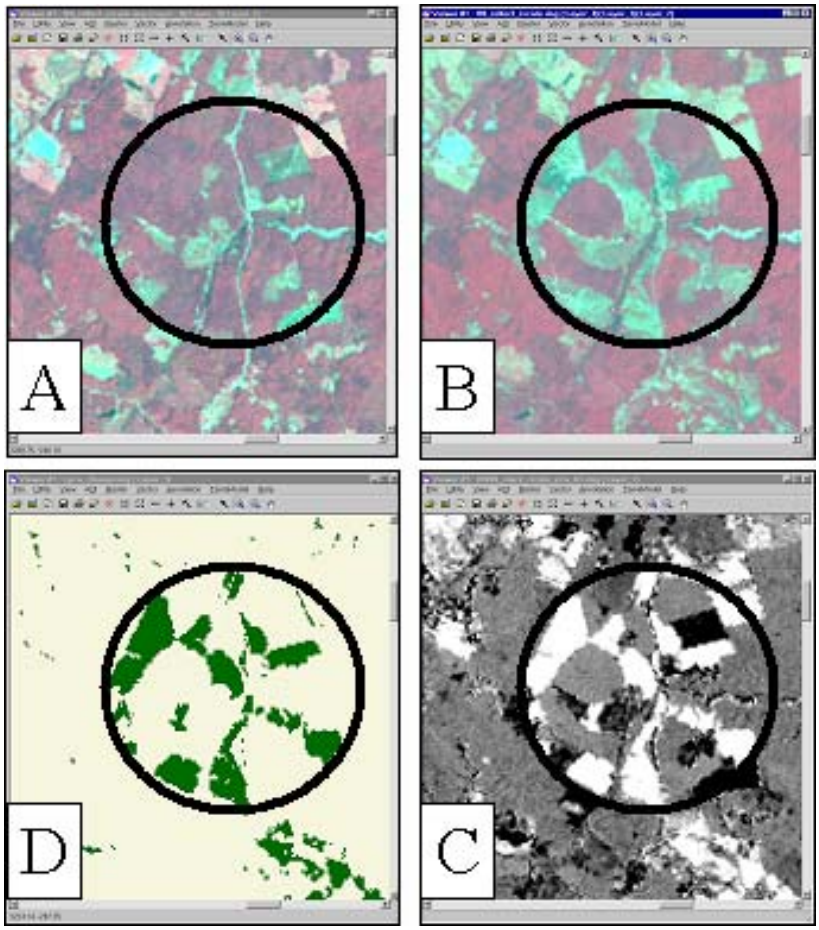

Figure 8 – Visual example of change detection using the SPCA technique.

35 and 345 differencing

The 345 method and 35 differencing methods were both developed by the Minnesota Department of Natural Resources, based on results from previous studies (Rack, 2002). TM band 3 is the red band, 4 is the near infrared band, and 5 is a mid infrared band. The 345 differencing method was designed to derive a cumulative difference based on bands sensitive to vegetation. This procedure was developed specifically for a study of aspen forests over a four-year period (Rack, 2002). The 35 differencing method was created as a remedy to the effect created by the difference in band 4 overwhelming others and missing cuts that had a fair time to regenerate. The 35 differencing method relied on the moisture measuring capabilities of middle infrared (Rack, 2002). Formulas for both methods are shown in Table 3.

Tasseled Cap Brightness and Greenness

The TCB and TCG methods use the tasseled cap transformation developed by Kauth and Thomas (1976). The tasseled cap transformation offers a way to optimize remotely sensed data for vegetation studies. Using the bands of Landsat TM, the transformation produces a set of new bands. The four bands that are created by a tasseled cap are listed below:

1. Brightness – weighted sum of all bands, it is defined in the direction of the principal variation in soil reflectance (Erdas, 1999).
2. Greenness – orthogonal to brightness, it is from the contrast between the near infrared band and the visible bands, and it is strongly related to the amount of green vegetation in the scene (Erdas, 1999).
3. Wetness – related to canopy and soil moisture (Lillesand and Kiefer, 1987).
4. Nonesuch – carries system noise and atmospheric information (Campbell, 1996).

The tasseled cap transformation is a linear transformation using remotely sensed data to project soil and vegetation information into multispectral data space (Campbell, 1996). Since the first two bands (TCB and TCG) usually convey most of the information present in a scene, they were chosen for this study. Although intended for agricultural use, these methods can be applied to forestry studies as well. In this method a tasseled cap transformation was performed on both images. For the TCB method, the brightness image (TC1) for the 1994 image was subtracted from the brightness image of 1998. The same method was used for the TCG technique using the greenness (TC2) image.

SPCA and PC1 Differencing

PC1 and SPCA both take advantage of the powerful PCA transformation. Positive correlations between bands indicate that the value of one band may be predicted by the values of the other bands (Faust, 1989). The ability to create a few images that represent most of the information held in many images (data reduction) is one very important use of PCA.

Principal components are the eigenvectors of a similarity matrix (usually a covariance or a correlation matrix). A covariance matrix represents all of the variance and covariance between the spectral bands in an image. PCA produces a transformation of a similarity matrix that generates new composite variables formed from linear combinations of the original variables. These new variables are calculated to remove dependencies that were reflected in the original variance/covariance structure. There are multiple output bands from a PCA, but the first few bands account for most of the variance in the data set (Erdas Field Guide, 1999; Davis, 1986). The bands of a PCA are non-correlated, independent, and often are more interpretable than the original source data (Jensen, 1996; Faust, 1989).

To run a PCA transformation, a linear transformation is performed on the data. The coordinates of each pixel in spectral space are recomputed using a linear equation (Erdas Field Guide, 1999). The result of the transformation is that the axes in n-dimensional spectral space are shifted and rotated relative to the axes of the ellipse (Erdas Field Guide). The first axis represents the direction of maximum variance in n-dimensional space (Davis, 1986; Faust, 1989). The other axes will be smaller than the previous ones, and will be oriented perpendicular to previous axes - evidence of the independence of each axis from the others. The PC transformation is known as a Karhunen-Loeve transform. It begins by calculating the covariance matrix for the total scene (Faust, 1989); the eigenvectors and eigenvalues must be derived from the covariance matrix to perform the linear transformation.

$$E \, Cov \, E^T = V$$

Where:
Cov = the covariance matrix,
E = the matrix of eigenvectors,
T = the transposition function, and
V = a diagonal matrix of eigenvalues, in which all nondiagonal elements are zeros.
V is computed so that its nonzero elements are ordered from greatest to least.
Source: Erdas Field Guide, 1999

The matrix, V, is the covariance matrix of the output principal component file. The zeros represent the covariance between bands (there is none), and the eigenvalues are ordered from largest to smallest. Each column of the resulting eigenvalue matrix describes a unit length vector in spectral space, which shows the direction of the PC (Faust, 1989); the numbers are used as coefficients in the following equation, to transform the original values into the PC values (Erdas Field Guide, 1999).

$$P_e = \sum_{k=1}^{n} d_k E_{ke}$$

Where:
e = the number of the principal component
P_e = the output principal component value for principal component band e
k = a particular input band
n = the total number of bands
d_k = an input data file value in band k
E = the eigenvector matrix, such that E_{ke} = the element of that matrix at row k, column e.
Source: Erdas Field Guide

For the PC1 differencing method, a PCA analysis was performed on each image separately, and then PC1 from the 1994 image was subtracted from PC1 of the 1998 image. The eigenvalues from the 1994 image are shown in Table 4. The data verifies that most of the variance (97.1%) in the scene is contained in the first two principal components. In Figure 9, we can observe this visually. Higher principal components (3-5) represent little variation; principal component 6 seems to represent system noise.

Table 4 – Eigenvalues for PCA performed on the 1994 image. The principal components bands are listed in descending order. PC1 contains most of the scene's variation (74.6%), and PC1 and PC2 combined contain 97.1% of the variation in the scene. Visual results from the PCA are shown in Figure 7.

PC	Variation	% Var.
1	452.12	74.6
2	136.51	22.5
3	12.46	2.1
4	2.52	0.4
5	1.92	0.3
6	0.69	0.1

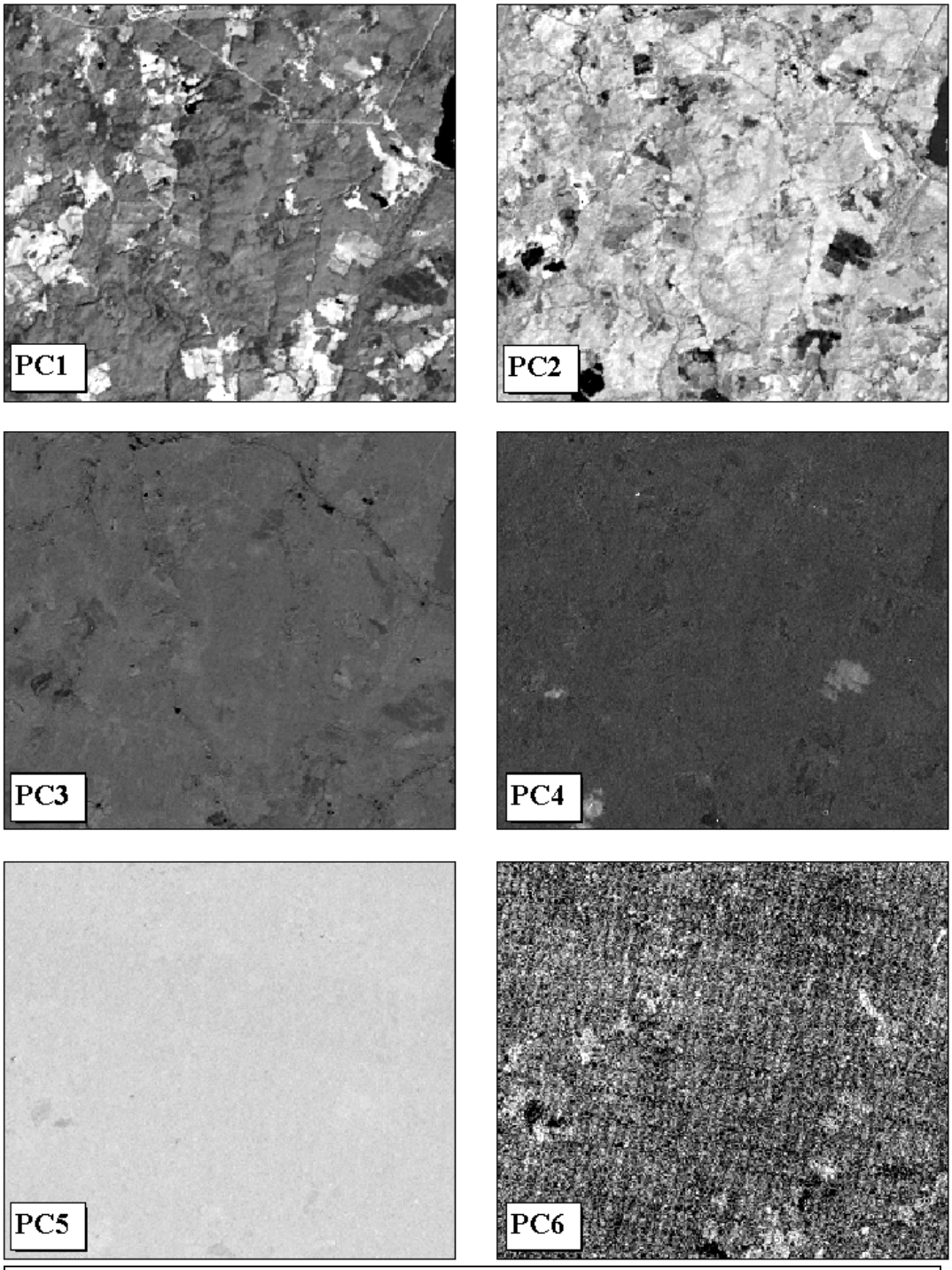

Figure 9 – Visual results from the PCA performed on the 1994 image.

For the SPCA method, the two six band images were stacked into a twelve band composite dataset. Then a PCA was performed on the composite set, and a "change band" was selected. In this case, PC3 was chosen as the change band.

Experiments have demonstrated that if the change occurs only on a small percentage of the study area, the first and second principal components tend to represent the unchanged land cover, while the third and later principal components contain the change information (Byrne et al, 1980; Richards, 1984; Lunetta, 1998)

NDVI Differencing

The NDVI image differencing technique makes use of the Normalized Difference Vegetation Index (NDVI). NDVI is one of a few vegetation indices developed to reduce multiple bands of data into a single number for each pixel that assess canopy characteristics such as biomass, productivity, leaf area index, and percent of vegetation ground cover (Jensen, 1996). Vegetation indices make use of the typical spectral characteristics of healthy green vegetation. Radiation in the red portion of the electromagnetic spectrum is absorbed by healthy vegetation while infrared radiation is strongly reflected. Rouse et al (1973) developed the NDVI on band ratioing using MSS data. The equation for performing an NDVI on Landsat TM data is shown below:

$$NDVI = \frac{TM4 - TM3}{TM4 + TM3}$$

Where:
TM3 = the red band
TM4 = the near infrared band

Figure 10 shows the results of performing an NDVI on the 1998 scene. The same area is shown on the left in a 432-band combination and on the right after a NDVI was performed. On the NDVI image, the bright areas indicate an abundance of healthy vegetation and dark areas indicate a lack of vegetation.

TM7 Differencing

Univariate differencing is the least mathematically complex of the change detection techniques, and simply involves subtracting a single band in one image from the same band in another image. TM band 7, a mid infrared band, was used for this study.

Mid infrared is extremely sensitive to plant moisture content, which is an overall indicator of tree health (Green and Cosentino, 1996; Lunetta, 1998).

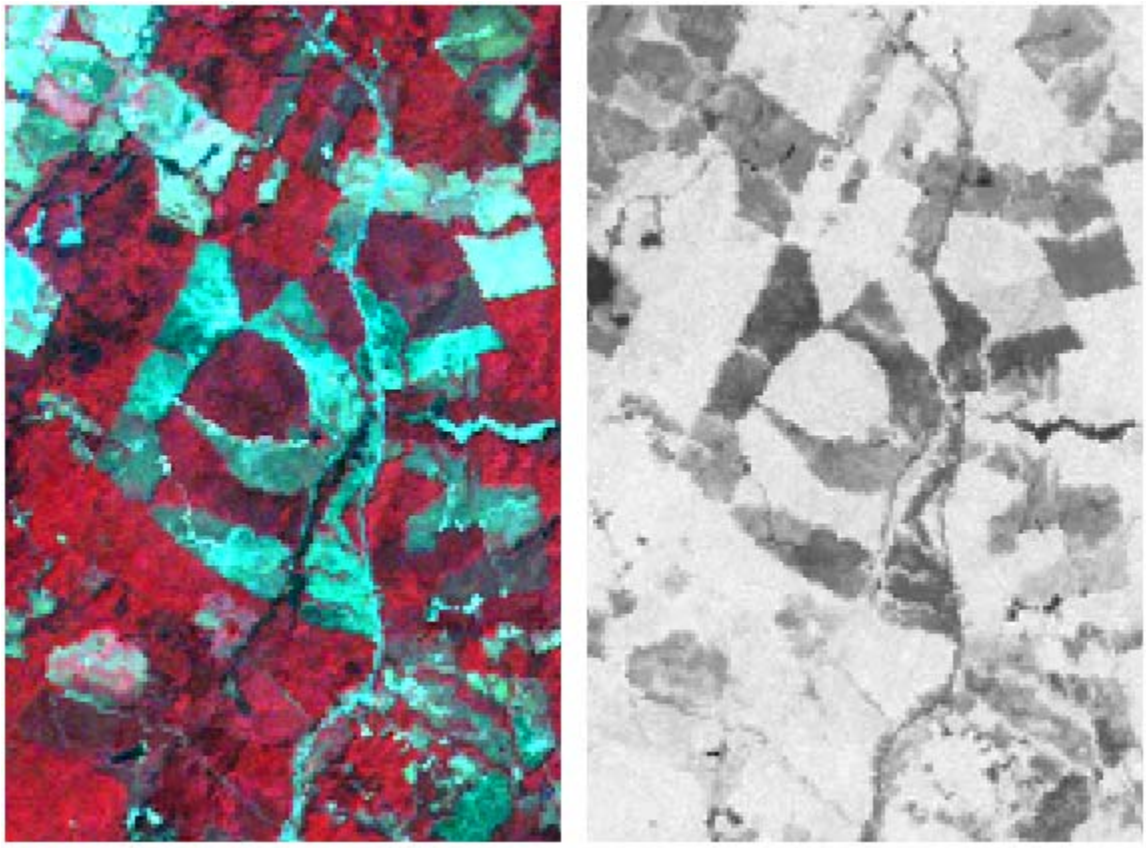

Figure 10 – Visual Example of an NDVI Performed on the 1998 Image.

5.7 Majority Filters

After the eight change detection techniques were performed, a majority filter was applied to each thematic change map to reduce the "salt and pepper" effect. The "salt and pepper" effect refers to small groups of misclassified pixels that are scattered throughout the change map. These could be due to small areas, not large enough to be considered harvested, where trees were removed. In this study the minimum size for harvested areas was 10 acres.

Filters function by passing a window over the pixels in the image. The center cell for the image is recalculated using the cell values within the window. In the case of majority filtering, the center cell is set to the majority value found in the window.

Filters using widow sizes of 3x3 pixels, 5x5 pixels, and 7x7 pixels were applied to the original dataset. The results of the majority filters were compared to the original change images to determine what affect they had on accuracy and the size of the different categories.

5.8 Hybrid Change Detection Technique

A hybrid method was designed to consider the results of the eight techniques discussed in the previous section. The goal was to increase accuracy and obtain additional information by using multiple techniques for the same study area. A model was developed using Erdas Imagine image processing software. First the thematic change maps from each of the eight change detection techniques were added together. Since the change maps were binary with a value of 1 classified non-harvested and a value of 2 classified harvest, the resulting "combined" or "stacked" image returned values ranging from 8 to 16. Table 5 gives the interpretation of the values in the combination image.

Pixel Value	Interpretation
8	All 8 methods = No harvest
9	1 of 8 methods = harvest
10	2 of 8 methods = harvest
11	3 of 8 methods = harvest
12	4 of 8 methods = harvest
13	5 of 8 methods = harvest
14	6 of 8 methods = harvest
15	7 of 8 methods = harvest
16	8 of 8 methods = harvest

Table 5 – Interpretation of values in the combination image.

The combined image can be observed in Figure 11. The pixel values have been divided into six categories for visual interpretation. Yellow areas are where the pixels were classified as non-harvested in all 8 methods, while blue areas were classified as non-harvest in all 8 methods. The combined image was thresholded multiple times so that eight change maps were produced. For example, one threshold was placed at the value 9, and if values were less than 9 they were coded as non-harvested, and values 9

and greater were coded as harvested. In other words, if at least 1 method classified a pixel as harvested, it was coded as harvest for the new image. Similar thresholds were placed at values 10-16. The resulting images were visually compared and an accuracy assessment was performed on each.

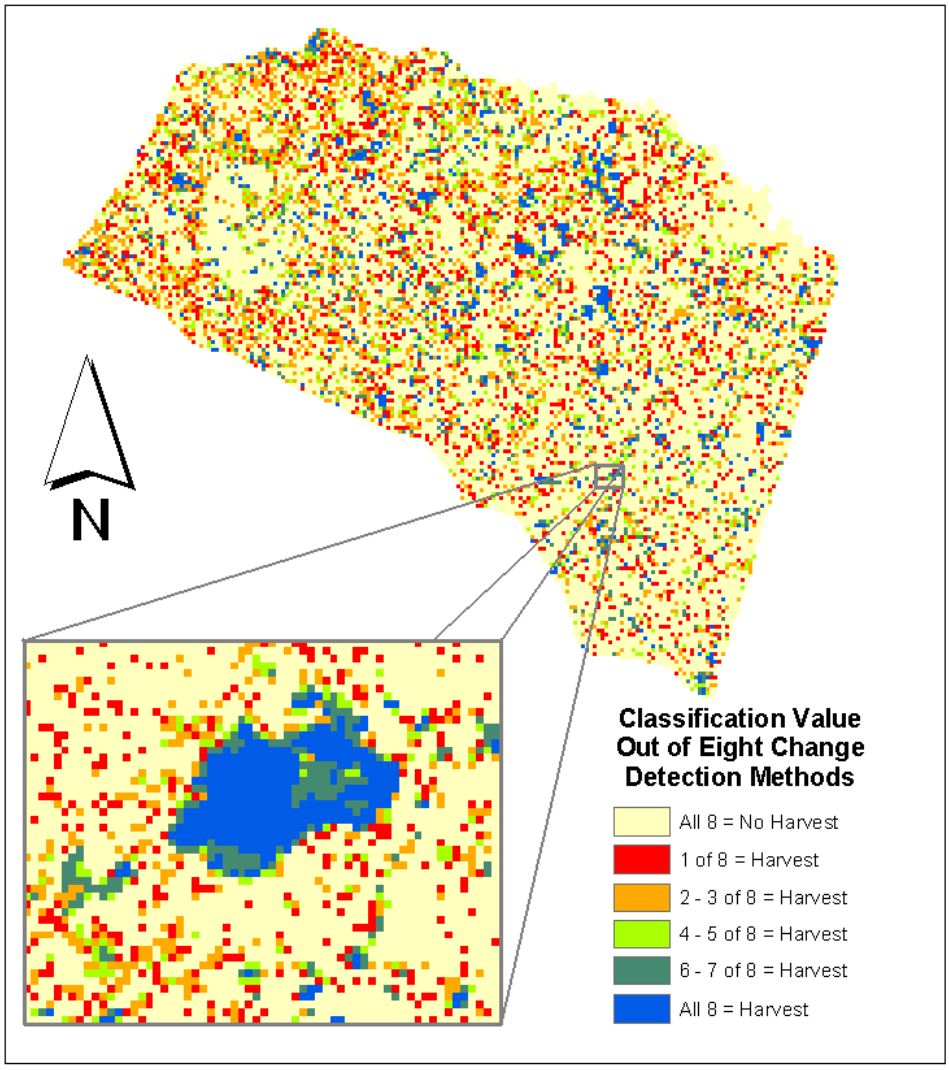

Figure 11 - Combination image created by stacking eight change maps.

5.9 Accuracy Assessment

The accuracy of the images was assessed using an error (contingency) matrix. An error matrix is used in most change detection and image classification studies. Overall accuracy, producers accuracy, users accuracy, errors of omission, errors of

commission, estimates of Kappa (Khat), Kappa variance, and Z-scores all can be derived from the error matrix.

Overall accuracy is the sum of the correctly classified points (diagonals) divided by the total number of reference points assessed. Errors of omission include areas that are omitted, for example an area of harvest on the ground was assigned to non-harvested category, so relative to the harvest category it was omitted. Therefore if a non-harvest pixel was assigned to harvest, it would be a commission error relative to the harvest category. The two categories have an inverse relationship, and are balanced by compensating errors. For producer's accuracy the assessment is based on the reference points, while the users (consumers) accuracy forms a guide to the reliability of the map as a predictive device.

Khat is an estimate of the actual agreement minus the chance agreement (Rutchey and Vilcheck, 1994). It indicates the degree of improvement over a random classification. A value of one would indicate perfect agreement, a value of zero would indicate pure chance, and any negative number up to negative one would indicate that the outcome was worse than what chance alone would give. Table 5 gives interpretation of Khat values. The value of using Khat in addition to overall accuracy is that it uses information from the entire error matrix while overall accuracy considers the diagonals only.

KHAT value	Agreement
> 0.80	Strong
0.4 – 0.8	Moderate
< 0.4	Poor

Table 6 - Interpretation of Khat values (Congalton and Green, 1999)

Z scores were used to determine if the methods were significantly different. Z-scores can either test change detection significance, or compare the difference between two change detection methods (Congalton and Green, 1999). If the Z-score is higher than 1.96 then it

is significantly different at the 95% confidence level than a random change detection, or two change detection products are significantly different from each other.

6. RESULTS

6.1 Comparison of Techniques

The eight techniques were performed on the raw data, and evaluated using an error matrix. Values of the overall accuracy ranged from 78.9 to 90.6, a span of 11.72 percent. The techniques ranked by overall accuracy and Khat in descending order are shown in table 6. TM7, which is the simplest algorithm mathematically, returned the best results. The overall accuracy for TM7 was 90.63%. PC1 differencing also returned good results with an overall accuracy of 89.06%. The 35, TCB, and 345 methods all performed admirably with overall accuracies of 87.50%, 87.11%, and 86.33%. Using the SPCA method, the third principal component was found to contain the change information. However SPCA performed lower than many of the other methods, with an overall accuracy of 83.59%. NDVI differencing performed poorly, with an overall accuracy of 82.81%. TCG was the worst performer and only achieved a 78.91% overall accuracy.

Rank	Method	Overall Accuracy	Khat
1	**TM7 differencing**	90.63	0.8113
2	**PC1 differencing**	89.06	0.7793
3	**35 differencing**	87.5	0.7505
4	**TCB differencing**	87.11	0.7436
5	**345 differencing**	86.33	0.7263
6	**SPCA**	83.59	0.6789
7	**NDVI differencing**	82.81	0.6578
8	**TCG differencing**	78.91	0.5836

Table 7 – The eight change detection techniques ranked by overall accuracy and Kappa scores.

The contingency matrix for each technique is shown in Table 8. Class 1 is harvested (clearcut), and Class 2 is non-harvested. User's Accuracy and Producer's accuracy for each class is shown. The column diagonals show the number of correctly classified pixels for each class. The 256 validation points were used to perform accuracy assessments.

345

	Class1	Class2	Row tot	**Users**
Class 1	101	26	127	79.53%
Class 2	9	120	129	93.02%
Col Tot	110	146	256	
Producers	91.82%	82.19%		

35

	Class1	Class2	Row tot	**Users**
Class1	104	26	130	80.00%
Class2	6	120	126	95.24%
Col Tot	110	146	256	
Producers	94.55%	82.19%		

NDVI

	Class1	Class2	Row tot	**Users**
Class1	99	33	132	75.00%
Class2	11	113	124	91.13%
Col Tot	110	146	256	
Producers	90.00%	77.40%		

PC1

	Class1	Class2	Row tot	**Users**
Class1	101	19	120	84.17%
Class2	9	127	136	93.38%
Col Tot	110	146	256	
Producers	91.82%	86.99%		

SPCA

	Class1	Class2	Row tot	**Users**
Class1	108	40	148	72.97%
Class2	2	106	108	98.15%
Col Tot	110	146	256	
Producers	98.18%	72.60%		

TCB

	Class1	Class2	Row tot	**Users**
Class1	105	28	133	78.95%
Class2	5	118	123	95.93%
Col Tot	110	146	256	
Producers	95.45%	80.82%		

TCG

	Class1	Class2	Row tot	**Users**
Class1	98	42	140	70.00%
Class2	12	104	116	89.66%
Col Tot	110	146	256	
Producers	89.09%	71.23%		

TM7

	Class1	Class2	Row tot	**Users**
Class1	104	18	122	85.25%
Class2	6	128	134	95.52%
Col Tot	110	146	256	
Producers	94.55%	87.67%		

Table 8 – Contingency matrices for each of the eight methods.

The contingency matrices for the methods were compared to determine if the methods were significantly different at the $\alpha = 0.05$ significance level. Scores higher than 1.96 are considered significantly different. As seen in Table 9, very few of the methods met this criterion. However this may be misleading, and most likely the low Z-scores are due to the fact that binary (harvest/non-harvest) images are being compared.

	345	**35**	**NDVI**	**PC1**	**SPCA**	**TCB**	**TCG**	**TM7**
345	0.00	0.34	-0.87	0.76	-0.63	0.24	-1.72	1.27
35	-0.34	0.00	-1.21	0.43	-0.98	-0.10	-2.05	0.94
NDVI	0.87	1.21	0.00	1.62	0.26	1.12	-0.85	2.12
PC1	-0.76	-0.43	-1.62	0.00	-1.40	-0.53	-2.46	0.51
SPCA	0.63	0.98	-0.26	1.40	0.00	0.88	-1.13	1.92
TC1	-0.24	0.10	-1.12	0.53	-0.88	0.00	-1.96	1.04
TC2	1.72	2.05	0.85	2.46	1.13	1.96	0.00	2.94
TM7	-1.27	-0.94	-2.12	-0.51	-1.92	-1.04	-2.94	0.00

Table 9 – Z-scores comparing change detection techniques

6.2 Majority Filters

After binary thematic harvest (harvest / no harvest) images were created from the raw imagery, majority filters were applied to eliminate the "salt and pepper" effect, which is caused by single or small groups of pixels that are misclassified as harvested. The smallest area that was considered harvested in this study was 10 acres. 3x3, 5x5, and 7x7 window sizes were applied to each of the eight thematic maps, which were then evaluated for accuracy.

				Class 1 -Non-harvest		Class 2 -Harvest	
	Technique and Window Size	**Overall Accuracy**	**Kappa**	**Producer's Accuracy**	**User's Accuracy**	**Producer's Accuracy**	**User's Accuracy**
1	**345 (none)**	86.33	0.7263	91.82	79.53	82.19	93.02
2	**345 (3x3)**	86.33	0.7275	93.64	78.63	80.82	94.40
3	**345 (5x5)**	86.33	0.7292	96.36	77.37	78.77	96.64
4	**345 (7x7)**	83.59	0.6782	97.27	73.29	73.29	97.27
5	**35 (none)**	87.50	0.7505	94.55	80.00	82.19	95.24
6	**35 (3x3)**	88.28	0.7661	95.45	80.77	82.88	96.03
7	**35 (5x5)**	89.06	0.7817	96.36	81.51	83.56	96.83
8	**35 (7x7)**	86.33	0.7298	97.27	76.98	78.08	97.44
9	**NDVI (none)**	82.81	0.6578	90.00	75.00	77.40	91.13
10	**NDVI (3x3)**	83.59	0.6761	94.55	74.29	75.34	94.83
11	**NDVI (5x5)**	82.81	0.6629	96.36	72.60	72.60	96.36
12	**NDVI (7x7)**	79.30	0.5970	95.46	68.63	67.12	95.15
13	**PC1 (none)**	89.06	0.7793	91.82	84.17	86.99	93.38
14	**PC1 (3x3)**	89.45	0.7879	93.64	83.74	86.30	94.74
15	**PC1 (5x5)**	90.23	0.8040	95.45	84.00	86.30	96.18
16	**PC1 (7x7)**	89.06	0.7817	96.36	81.54	83.56	96.83
17	**SPCA (none)**	83.59	0.6789	98.18	72.97	72.60	98.15
18	**SPCA (3x3)**	83.59	0.6789	98.18	72.97	72.60	98.15
19	**SPCA (5x5)**	80.86	0.6282	98.18	69.68	67.81	98.02
20	**SPCA (7x7)**	78.13	0.5774	97.27	66.88	63.70	96.88
21	**TC1 (none)**	87.11	0.7436	95.45	78.95	80.82	95.93
22	**TC1 (3x3)**	87.89	0.7591	96.36	79.70	81.51	96.75
23	**TC1 (5x5)**	87.11	0.7458	99.09	77.37	78.08	99.13
24	**TC1 (7x7)**	84.83	0.6936	98.18	73.97	73.97	98.18
25	**TC2 (none)**	78.91	0.5836	89.09	70.00	71.23	89.66
26	**TC2 (3x3)**	78.91	0.5854	90.91	69.44	69.86	91.07
27	**TC2 (5x5)**	77.34	0.5576	91.82	67.33	66.44	91.51
28	**TC2 (7x7)**	76.95	0.5504	91.82	66.89	65.75	91.43
29	**TM7 (none)**	90.63	0.8113	94.55	85.25	87.67	95.52
30	**TM7 (3x3)**	90.23	0.8040	95.45	84.00	86.30	96.18
31	**TM7 (5x5)**	90.63	0.8125	97.27	83.59	85.62	97.66
32	**TM7 (7x7)**	89.45	0.7898	97.27	81.68	83.56	97.60

Table 10 – Overall accuracy, Khat, and categorical User's and Producer's accuracy for the eight techniques with filters applied.

As observed in Table 10, the 3x3 and 5x5 window sizes raised overall accuracy and Kappa statistics in most cases. The majority filter with a 3x3 window increased the overall accuracy compared to the original change map in six cases, and stayed the same in one case. Overall accuracy declined only for the TM7 technique. The 5x5 window increased overall accuracy compared to the original change map in six cases, and experienced a decline in the TCG and the SPCA methods. The majority filter using a 7x7 window degraded overall accuracy compared to the original change map in all cases except for PC1 where it returned the same overall accuracy and a slightly higher kappa statistic.

Although the overall accuracy values were relatively consistent when the majority filters were applied, the individual categorical accuracy changed significantly. For example, using the 345 technique, overall accuracy stays the same for the original change map when the 3x3 and 5x5 majority filters are applied. However, producer's accuracy in the non-harvest category increases significantly, and producer's accuracy for the harvested area decreases. The general trend is that when majority filters of increasing window sizes are applied to the change map, a marked increase in Producer's accuracy for the non-harvested area and a decrease in Producer's accuracy for harvested areas are observed. Compensating fluctuations in User's accuracy occur as well.

Table 11 shows the change in acreage and percentages for each category in the change maps. The maps with the majority filters applied lost large amounts of area in the clearcut category. Since the majority of the study area experienced no harvest it is logical that the application of majority windows would cause a decrease in the category with the least area. However, with the application of the 3x3 window area in the harvested category decreased an average of 5.95%. The TCG method showed a decrease of 7.4% in harvested area when the 3x3 filter was applied. When the window size was increased to 7x7, area for the harvested category dropped an average of 9.59%, as much as 11.3% for the TCG method.

Technique	Non-Harvest Acres	Harvested Acres	Percent Non-Harvest	Percent Harvested
35 (no filter)	266727.0	49984.4	84.2	15.8
35 (3x3 majority)	286223.9	30487.4	90.4	09.6
35 (5x5 majority)	294020.9	22690.5	92.8	07.2
35 (7x7 majority)	297631.2	19080.1	94.0	06.0
345 (no filter)	272668.8	44042.6	86.1	13.9
345 (3x3 majority)	288759.9	27951.5	91.2	08.8
345 (5x5 majority)	295908.6	20802.8	93.4	06.6
345 (7x7 majority)	299366.1	17345.2	94.5	05.5
NDVI (no filter)	263957.5	52753.8	83.3	16.7
NDVI (3x3 majority)	282294.7	34416.7	89.1	10.9
NDVI (5x5 majority)	290720.8	25990.6	91.8	08.2
NDVI (7x7 majority)	295202.9	21508.5	93.2	06.8
PC1 (no filter)	260381.9	56329.5	82.2	17.8
PC1 (3x3 majority)	279803.6	36907.8	88.3	11.7
PC1 (5x5 majority)	289065.7	27645.7	91.3	08.7
PC1 (7x7 majority)	293688.0	23023.4	92.7	07.3
SPCA (no filter)	281012.8	35698.6	88.7	11.3
SPCA (3x3 majority)	297268.3	19443.1	93.9	06.1
SPCA (5x5 majority)	301934.4	14777.0	95.3	04.7
SPCA (7x7 majority)	303946.6	12764.8	96.0	04.0
TCB (no filter)	263500.1	53211.3	83.2	16.8
TCB (3x3 majority)	286899.1	29812.3	90.6	09.4
TCB (5x5 majority)	295706.0	21005.4	93.4	06.6
TCB (7x7 majority)	299374.6	17336.8	94.5	05.5
TCG (no filter)	255939.3	60772.9	80.8	19.2
TCG (3x3 majority)	274008.2	42703.1	86.5	13.5
TCG (5x5 majority)	283673.3	33038.1	89.6	10.4
TCG (7x7 majority)	288900.5	27810.9	91.2	08.8
TM7 (no filter)	271066.4	45645.0	85.6	14.4
TM7 (3x3 majority)	290329.6	26381.8	91.7	08.3
TM7 (5x5 majority)	297225.6	19485.8	93.8	06.2
TM7 (7x7 majority)	300037.6	16673.8	94.7	05.3

Table 11 – The effect of majority filters on class size.

Visually, the majority filters did a good job of eliminating the "salt and pepper" effect of the images. Figure 12 illustrates the difference between the change maps created using the original image with no filters, and majority filters using three window sizes. Figure 12a, a subset of the change map created from the TM7 technique, was subjected to filtering. The change images created using the 3x3 (Figure 12b), 5x5 (Figure 12c), and 7x7 (Figure 12d) window sizes are shown. The green areas on the image represent those pixels that were classified as clearcuts. As window sizes increase, more of the scattered harvest pixels are eliminated.

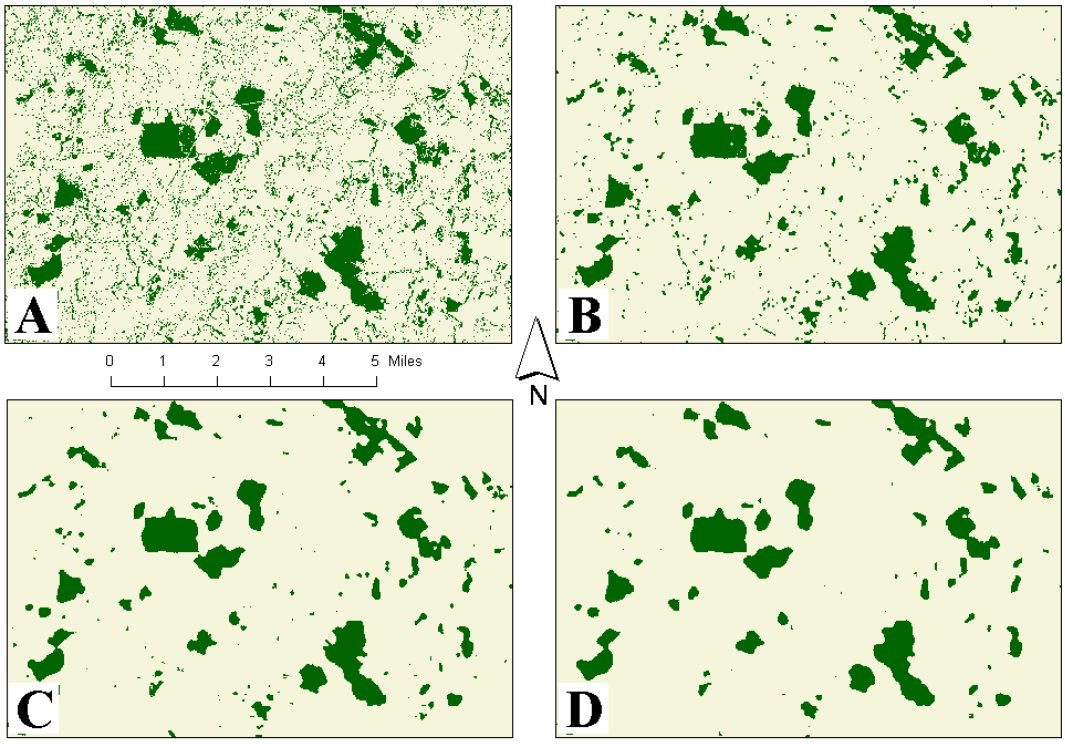

Figure 12 – A visual comparison of the effects of applying majority filters.

6.3 Atmospheric Corrections

Seven methods performed on the three input sets were evaluated using overall accuracy (Table 12). Of the three levels of corrections, the change detection algorithms performed on the images converted to reflectance returned the best results with an average overall accuracy of 85.16%. However, the raw (original) images had results with an average overall accuracy of 85.04%, so the overall gains in accuracy were not significant. The images converted to reflectance and corrected for

atmospheric errors had the lowest overall accuracy of 82.48%, which is a significant degradation of accuracy. These results would tend to agree with studies by Song et al (2001) that the more complex atmospheric correction algorithms do not necessarily lead to improved performance of change detection algorithms.

Technique by technique comparisons can also be made. The 345 differencing method received similar results using the raw imagery, and the atmospherically corrected imagery. The 35 differencing method improved when corrections were applied. The NDVI method improved when the images were converted to reflectance, but was degraded when the atmospheric corrections were applied. PC1 and TCB methods both experienced a loss in accuracy. The conversion to reflectance increased accuracy over the raw imagery in four cases, and decreased accuracy in three. The atmospheric corrections increased accuracy over the raw imagery in one case, returned the same results in another, and decreased accuracy in the other cases.

IMAGE SET	345	35	NDVI	PC1	SPCA	TCB	TCG
RAW	86.33	87.5	82.81	89.06	83.59	87.11	78.91
REFLECTANCE	85.94	88.28	85.16	85.16	86.33	85.94	79.3
ATMOSPHERIC	86.33	88.28	78.52	76.56	84.77	84.38	78.52

Table 12 – Comparison of the impact of atmospheric corrections on overall accuracy.

6.4 Hybrid Change Detection Technique

A hybrid change detection technique using the change maps from the eight change techniques was designed and implemented using Erdas Imagine image processing software.

The first step of the process was to merge the eight change maps into one "combination" image by adding the maps together. The new categories of the resulting image (Figure 11) are given in Table 13 along with the number of pixels, acreage, and percent of the total area for each. 62.4% (197,589 acres) of the image was classified as non-harvest by all 8 methods while only 4.0% (12,688 acres) was classified as harvest by all 8 methods. The non-forest mask that automatically caused 26.6% (84,147 acres) of the image to be classed as non-harvest in every technique

increased the amount no-harvest pixels for each method. Otherwise uncertainty would be much higher. Even with the non-forest mask applied, 33.6 % (106,434 acres) of the image was classed differently according to which change detection technique was used.

Category	No. Pixels	Acres	Percent
No Harvest	888462	197589.37	62.4
1 of 8 Harvest	157771	35087.46	11.1
2 of 8 Harvest	110979	24681.16	07.8
3 of 8 Harvest	70378	15651.70	04.9
4 of 8 Harvest	42722	9501.15	03.0
5 of 8 Harvest	33742	7504.05	02.4
6 of 8 Harvest	36224	8056.03	02.5
7 of 8 Harvest	26765	5952.40	01.9
8 of 8 Harvest	57052	12688.07	04.0
Totals	**1424095**	**316711.4**	**100.0**

Table 13 – Information about the categories in the combination image.

The next step of the process involved thresholding the images, and performing an accuracy assessment. The area for each category and the results of the overall accuracy for the thresholds applied to the combination image are shown in Table 14. Thresholds ranging from 2+ to 6+ gave good results with accuracies ranging from 85.16% to 90.63%, the highest accuracy being obtained when pixels that were classified harvest at least 3 times out of 8 methods was recoded harvest. The thresholds of 8 out of 8 methods returned the lowest overall accuracy (72.27%). 37.6% of the image (119122 acres) was classified as clearcut in at least one of the eight methods, while only 4% (12688 acres) was classed as clearcut for all 8 methods. The method with the highest accuracy, 3 of 8 methods, returned 18.7% (59353 acres) harvested.

Technique	Non-Harvest Acres	Harvested Acres	Percent Non-Harvest	Percent Harvested	Overall Accuracy	Khat
1+ methods	197589.4	119122.0	62.4	37.6	81.25	0.6041
2+ methods	232676.8	84034.6	73.5	26.5	87.50	0.7421
3+ methods	257358.0	59353.4	81.3	18.7	90.63	0.8104
4+ methods	273009.7	43701.7	86.2	13.8	90.23	0.8040
5+ methods	282510.8	34200.5	89.2	10.8	87.50	0.7511
6+ methods	290014.9	26696.5	91.6	08.4	85.16	0.7076
7+ methods	298070.9	18640.5	94.1	05.9	79.30	0.5996
All 8 methods	304023.3	12688.1	96.0	04.0	72.27	0.4758

Table 14 – Category information and accuracies for the hybrid method change maps.

7 CONCLUSIONS

In this study change detection using Landsat TM was successful in detecting forest harvesting. This study concludes that the TM7 differencing technique seems an effective tool for identification of forest harvests. Out of the methods used TM7 was the most accurate, as well as the simplest algorithm mathematically. This conclusion agrees with that of Green and others (1994). The PC1 differencing technique performed admirably, only slightly less accurate than the TM7 technique. The 35, TCB, and 345 techniques also provided good results.

The use of the original imagery seems to return suitable results without any further corrections applied. The conversion to reflectance did not degrade overall accuracy, and actually gave higher results in four of the seven change detection methods. The atmospheric correction of the images actually decreased harvest detection accuracy, and should only be considered if the images have major atmospheric errors. Further considerations when applying the atmospheric and radiometric corrections should include the time involved, the increase in file sizes (Table 15), rescaling the data, etc. With data sets that have atmospheric problems, then the corrections may improve the accuracy, however, if the data set is of good quality the added time and effort may need to be considered.

Year	Raw	Reflectance	Atmospheric
1994	17.6	64.6	70.2
1998	16.2	64.6	70.3

Table 15 – A comparison of file sizes for the three image sets.

The majority filters were effective in eliminating the "salt and pepper" effect of the images. The visual appearance of the change map is improved, single and small groups of pixels are eliminated, and large contiguous areas remain. However, the total area in the harvest category decreased significantly when majority filters were applied. Window sizes of 3x3 and 5x5 slightly increased or decreased overall accuracy in most cases, but a large shift in Producer's and User's accuracy was

observed. The 7x7 window size is not recommended because of its clearly negative affect on accuracy.

Even though the increased complexity of using the hybrid model involves performing multiple change detections and further analysis, to address fuzziness between change detection techniques, this routine is a valuable tool. This hybrid method is useful for identifying trends in the data as well as areas of certainty and uncertainty.

8 DISCUSSION

Sources of error in the performance of change detection include data acquisition, processing, analysis, and conversion. Accuracy is more complex for a change detection exercise than a single image classification accuracy assessment. Error sources that affect the accuracy of a single image in an analysis will contribute errors to the change detection accuracy (Dia & Khorram, 1998).

The accuracy of change detection methods can be influenced by atmospheric conditions. Atmospheric corrections attempt to eliminate optical distortions and normalize the imagery. However the additional time and effort needed to correct the images should be weighed against the gains in accuracy they will produce. In this study, the results of the atmospheric corrections varied from method to method, and are likely to vary with different data sets as well.

Misregistration is one significant source of error for multitemporal change detection techniques. A root mean square error (RMSE) less than 0.2 pixels is needed for a change detection error less than 10% (Dia & Khorram, 1998). Most change detection techniques are performed on a pixel-by-pixel basis and require accuracy of geometric registration for the two images. Although the RMSE for this project was within acceptable standards for both images, even slight registration errors could affect the boundaries between classes. Since many of the validation points used in the accuracy assessment were sampled near boundaries, reported accuracies may have been underestimated.

One impediment to the operational use of image differencing and related spectral change detection techniques is the subjective thresholding of the change image. The selection of a threshold is likely to differ from analyst to analyst. A C++ program has been created that uses a repeatable and objective method of finding thresholds based upon pre-specified criterion (Wynne and Scrivani, 2000). The program requires that

the change maps be converted to another file format. Due to the large quantities of maps produced in this study, and the time and effort required to convert the maps to another format, the program was not used for this study. The thresholds in this study were chosen by a visual inspection of both images to locate areas of forest harvesting. The areas found to be harvested were then used on the image after the algorithm was applied, and sampling of the area was used to establish thresholds. A range of threshold values was applied to the image, and the one with the highest overall accuracy were used. Although this method was constant for this study, different results may be obtained from different analysts. A separate program or additional tool designed to work with files in a format native to Erdas Imagine should be developed. It would be helpful if the program had a slide bar that could be adjusted for different threshold values, and overall, Producer's, and User's accuracy could be automatically updated.

Uncertainty can be attributed to numerous factors when dealing with digital change detection. Measurement procedures generally produce data with limited accuracy, which leads to uncertainty. When temporal information is used to analyze change, these uncertainties will influence the final results (Cheng, 2002). For example, pixels are treated as though they have crisp boundaries when in reality the boundaries are indeterminate and the spatial extent is fuzzy. For example, although medium resolution is very useful for studies of a regional scale, the relatively coarse resolution of Landsat TM data is a

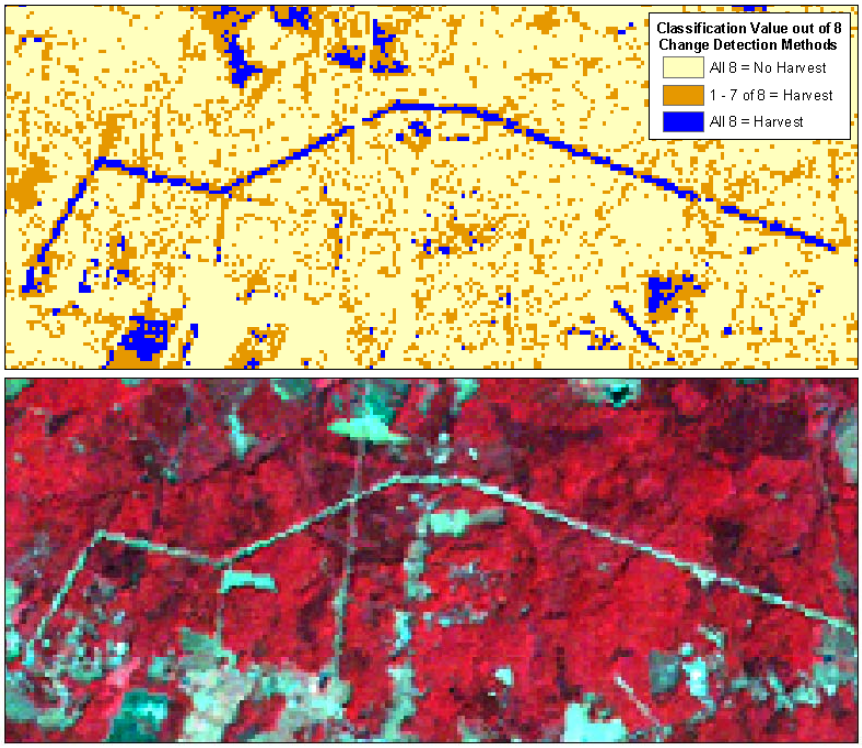

Figure 13 – Example of a misinterpreted area; the new road was classified as forest harvest.

disadvantage in some cases. For this exercise, each 30x30 meter pixel was classified as either harvested or non-harvested. Within the area that is encompassed by a pixel, there is a realistic chance that only partial harvesting occurred. Therefore the decision to label a pixel harvested or not may be misleading. Mixed pixels on edges are fuzzy in nature, but since the classification was binary mixed pixels on edges that did not fit into the correct class, would decrease accuracy in the binary change / no-change image.

The presence of a non-forest mask helped with the classification techniques, and attributed to higher accuracy. Areas outside the non-forest mask that experienced clearing for purposes other than harvesting are indistinguishable from forest harvests. An example of this is illustrated in Figure 13. The bottom image in the Figure is a portion of the 1998 image. The road that runs generally East-West across the image was developed after the 1994 image was acquired. In the image on the top, yellow areas were classified as non-harvest in all cases, the orange areas were classified

harvest in at least one out of the eight methods, and the blue areas were classified harvest for all methods. Since forest was cleared, the top image shows that all of the change detection techniques in this study classified at least a portion of the road as harvested land. Although it is true that the forested land was cleared to develop the road, this change does not match our definition of forest harvesting. Change detection algorithms only distinguish spectral change, not the nature of the change in informational classes.

Other possible effects on the accuracy assessment include the location of the validation points as well as the method that the software (Erdas Imagine 8.4) used to perform accuracy assessments. For validation points it is common to pick homogenous areas and locate a point in the center, which inflates accuracy because edges are avoided and the effect of misregistration errors is minimized (Macleod & Congalton, 1998). In this study the validation points were sampled in both homogenous areas and on boundaries, so misregistration errors would affect accuracy more. In addition, the image processing software used in this study does not perform point-to-point accuracy assessment. Rather it performs a majority neighborhood algorithm using a 3x3 pixel window. Therefore accuracy of the images is probably much lower than if samples were taken in homogenous areas only.

9. WORKS CITED

Banner, A.V. (1991). Change Detection Using Commercial Satellite Imagery to Monitor Large-Scale Withdrawals of Conventional Forces. *Overhead Imaging for Verification and Peacekeeping: Three Studies,* The Arms Control and Disarmament Division, External Affairs and International Trade, Canada.

Banner, A.V. and T. Lynham (1981). Multitemporal Analysis of Landsat data for Forest Cut Over Mapping – a Trial of Two Procedures. *Proceedings of the 7th Canadian Symposium on Remote Sensing*, Winnipeg, pp. 233-240.

Bauer, M.E., E.B. Thomas, A.R. Ek, P.R. Coppin, S.D. Lime, T.A. Walsh, D.K. Walters, W. Befort and D.F. Heinzen (1994). Satellite Inventory of Minnesota Forest Resources. *Photogrammetric Engineering and Remote Sensing*, 60, 3, pp 297 –298.

Bernstein R., C. Colby, S.W. Murphery, and J.P. Snyder (1983). Image Geometry and Rectification. *Manual of Remote Sensing, 2nd Edition*. (D.S. Simonett and G.A. Thorly editors). Sheridan Press. Pp. 873-922.

Byrne, G.F., P.F. Crapper, and K.K. Mayo (1980). Monitoring Land-Cover Change by Principal Component Analysis of Multitemporal Landsat Data. *Remote Sensing of the Environment*, 10, pp. 175-184.

Campbell, J.B. (1996). *Introduction to Remote Sensing, 2nd ed*, The Guilford Press.

Cheng, T. (2002). Fuzzy Objects: Their Changes and Uncertainties. *Photogrammetric Engineering and Remote Sensing,* 68, 1, pp. 41-49.

Colwell, J.E. and F.P. Weber (1981). Forest Change Detection. *Proceedings of the 15th International Symposium on Remote Sensing of the Environment*, Ann Arbor, MI.

Dai, X. and S. Khorram (1998). The Effects of Image Misregistration on the Accuracy of Remotely Sensed Change Detection. *IEEE*, 5.

Davis, J.C. (1986). *Statistics and Data Analysis in Geology, 2nd ed*, John Wiley & Sons, Inc.

Deers, P.J. (1995). Digital Change Detection Techniques: Civilian And Military Applications. Information Technology Division, Defence Science and Technology Organisation, Australia, web document: http://ltpwww.gsfc.nasa.gov/ISSSR-95/digitalc.htm

Deitweiler, R.P., and C.A.S. Hall (1988). Tropical forests and the global carbon cycle. *Science*, 239, pp. 42-47.

Erdas (1999). *Erdas Field Guide, 5th ed*, Atlanta, GA. Erdas Inc.

Faust, N.L. (1989). Image Enhancement. *Encyclopedia of Computer Science and Technology* (A. Kent and G. Williams, editors), 20, 5.

Fung, T. and E. LeDrew (1988). The Determination of Optimum Threshold Levels for Change Detection. *Photogrammetric Engineering and Remote Sensing*, 54, 10, pp. 1449-1454.

Gildea, J.J. (2000). Relationships Between Land Use, Land Use Change, and Surface Water Quality Trends in Virginia. Masters Thesis, Virginia Polytechnic Institute and State University, Blacksburg.

Green, K.S. and B. Consentino (1996). Using Satellite Imagery to Detect and Monitor Forest Change. *Geo Info Systems*, 6,2, pp. 22-30.

Green, K.S., D.K. Kempka and L. Lackey (1994). Using Remote Sensing to Detect and Monitor Land-Cover and Land-Use Change. *Photogrammetric Engineering and Remote Sensing*, 60, 3, pp. 331-337

Hame, T., I Heiler, and J.S. Miguel-Ayanz (1998). An unsupervised change detection and recognition system for forestry. *International Journal of Remote Sensing*. 19, 6, pp. 1079-1099.

Hayes, D.J. and S.A. Sader (2001). Comparison of Change-Detection techniques for Monitoring Tropical Forest Clearing and Vegetation Regrowth in a Time Series. *Photogrammetric Engineering and Remote Sensing*. 67, 9, pp. 1067-1075.

Howarth, P.J. and G.M. Wickware (1981). Procedures for Change Detection Using Landsat Digital Data. *International Journal of Remote Sensing*, 2, pp. 277-291.

Jano, A.P., R.L. Jefferies and R.F. Rockwell (1998). The Detection of Vegetational Change by Multitemporal Analysis of Landsat Data: The Effects of Goose Foraging. *Journal of Ecology*, 86, 1, pp. 93-99.

Jensen, J.R. (1996). *Introductory Digital Image Processing; A Remote Sensing Perspective,* 2nd Edition. Prentice Hall, Inc.

Jensen, J.R., K. Rutchey, M.S. Koch, and S. Narumalani (1995). Inland Wetland Change Detection in the Everglades Water Conservation Area 2A Using a Time Series of Normalized Remotely Sensed Data. *Photogrammetric Engineering and Remote Sensing*, 61, 2, pp. 199-209.

Jiaju, L. (1988). Development of Principal Components Analysis Applied to Multitemporal Landsat TM Data. *International Journal of Remote Sensing*, 9, pp. 1895-1907.

Kauth, R.J. and G.S. Thomas (1976). The Tasseled Cap – A Graphic Description of the Spectral-Temporal Development of Agricultural Crops as Seen by Landsat. *In LARS: Proceedings of the Symposium on Machine Processing of Remotely Sensed Data*, West Lafayette, IN: Purdue University, pp. 4B-41 – 4B-51.

Lambin, E.F. and A.H. Strahler (1994). Change-vector Analysis in Multispectral Space: A Tool to Detect and Categorize Land-cover Change Processes Using High Temporal-resolution Satellite Data. *Remote Sensing of the Environment*, 48, pp. 231-244.

Lean, J. and D. Warilow (1989). Simulation of the regional climate impact of Amazon deforestation. *Nature*, 342, pp. 411-412.

Lillesand, T.M. and R.W. Kiefer (1987). *Remote Sensing and Image Interpretation*, New York: John Wiley & Sons, Inc.

Lugo, A.E. and S. Brown (1992). Tropical forests as sinks of atmospheric carbon. *Forest Ecology Management*, 54, 1, pp. 239-255.

Lunetta, R.S. (1998). Applications, Project Formulation, and Analytical Approach. *Remote Sensing Change Detection: Environmental Monitoring Methods and Applications* (R.S. Lunetta and C.D. Elvidge, editors), Ann Arbor Press, Chelsea, MI, pp. 1- 19

Lunetta, R.S., J.G. Lyon, B. Guindon, and C.D. Elvidge (1998). North American Landscape Characterization: "Triplicate" Data Sets and Data Fusion Products. *Remote Sensing Change Detection: Environmental Monitoring Methods and Applications* (R.S. Lunetta and C.D. Elvidge, editors), Ann Arbor Press, Chelsea, MI, pp. 41- 52

Lyon, J.G., D. Yuan, R.S. Lunetta, and C.D. Elvidge (1998). A change-detection experiment using Vegetation Indices. *Photogrammetric Engineering and Remote Sensing*, 64, 2, pp. 143-150.

Macleod, R.D. and R.G. Congalton (1998). A quantitative comparison of change-detection algorithms for monitoring eelgrass from remotely sensed data. *Photogrammetric Engineering and Remote Sensing*, 64, 3, pp. 207-216.

Malila, W.A. (1980). Change Vector Analysis: An Approach for Detecting Forest Change with Landsat. *Proceedings of the Annual Symposium on Machine Processing of Remotely Sensed Data*, *IEEE*, pp. 326-336.

Markham, B.L. and J.L. Barker (1985). Spectral characterization of the Landsat TM sensors. *International Journal of Remote Sensing*, 6, 5, pp. 697-716.

Martin, L.R.G. (1989). Accuracy Assessment of Landsat-Based Visual Change Detection Methods Applied to the Rural-Urban Fringe. *Photogrammetric Engineering and Remote Sensing*, 55, pp. 209 – 215.

Mas, J.F. (1999). Monitoring Land-Cover changes: A comparison of change detection techniques. *International Journal of Remote Sensing,* 20,1, pp.139-152.

Michener, W.K. and P.F. Houhoulis (1997). Detection of Vegetation Changes Associated with Extensive Flooding in a Forested Ecosystem. *Photogrammetric Engineering and Remote Sensing*, 63, 12, pp. 1363-1374.

Muchoney, D.M. and B.N. Haack (1994). Change Detection for Monitoring Forest Defoliation. *Photogrammetric Engineering and Remote Sensing*, 60, pp. 1243-1251.

Nelson, R.F. (1983). Detecting Forest Canopy Change Due to Insect Activity Using Landsat MSS. *Photogrammetric Engineering and Remote Sensing*, 49, pp. 1303-1314.

Price, J.C. (1987). Calibration of satellite radiometers and the comparison of vegetation indexes. *Remote Sensing of Environment*. 21, 1, pp. 15-27.

Raabe, E.A. and R.P. Stumpf (1997). Image Processing Methods; Procedures in Selection, Registration, Normalization and Enhancement of Satellite Imagery in Coastal Wetlands. *USGS Open File Report, 97-287*.

Rack, J. (2002). Personal communication.

Richards, J.A. (1984). Thematic Mapping from Multitemporal Image Data Using the Principal Components Transformation. *Remote Sensing of Environment*, 16, pp. 35-46.

Roberts, D.A., G.T. Batista, J.L.G. Pereira, E.K. Waller, and B.W. Nelson (1998). Change Identification Using Multitemporal Spectral Mixture Analysis: Applications in Eastern Amazonia. *Remote Sensing Change Detection: Environmental Monitoring Methods and Applications* (R.S. Lunetta and C.D. Elvidge, editors), Ann Arbor Press, Chelsea, MI, pp. 137- 161

Rouse, J.W., R.H. Haas, J.A. Schell, and D.W. Deering (1973). Monitoring Vegetation Systems in the Great Plains with ERTS. *Proceedings, 3rd ERTS Symposium*. 1, pp. 48-62.

Sader, S.A. (1995) Spatial Characteristics of Forest Clearing and Vegetation Regrowth as Detected by Landsat Thematic Mapper Imagery. *Photogrammetric Engineering and Remote Sensing*, 61, 9, pp. 1145-1151.

Scrivani, J.A. (2000). Speech at the Virginia Division SAF Summer Meeting. Lynchburg, Virginia. June 9.

Skole, D. and C. Tucker (1993). Tropical deforestation and habitat defragmentation in the Amazon: satellite data from 1978 to 1988. Science, 260, pp. 1905-1910.

Shukla, J., C. Nobre, and P. Sellers (1990). Amazon deforestation and climate change, *Science*, 247, pp. 1322-1325.

Singh, A. (1989). Digital Change Detection Techniques Using Remotely Sensed Data. *International Journal of Remote Sensing*, 10, pp. 989-1003.

Singh, A. (1986). *Change Detection in the Tropical Forest Environment of Northeastern India Using Landsat. Remote Sensing and Tropical Land Management*, (M.J. Eden and J.T. Parry editors), John Wiley & Son, Inc. pp. 237-254.

Sloggett, D., C. Gurney, W. Newton, R. Gooding and I. Dowman (1994). An Automated Change Detection System. *Proceedings of the 1994 International Geoscience and Remote Sensing Symposium*, pp. 875-877.

Song, C., M.P. Lenney, S.A. Macomber, C.E. Woodcock and K.C. Seto (2001). Classification and Change Detection using Landsat TM Data: When and how to Correct Atmospheric Effects? *Remote Sensing of the Environment,* 75, 2, pp. 230 –244.

Stow, D.A., D. Collins, and D. McKinsey (1990). Land Use Change Detection Based on Multi-date Imagery from Different Satellite Sensor Systems. *Geocarto International*, 5, pp. 3-12.

Stow, D.A., L.R. Tinney, and J.E. Estes (1980). Deriving Land Use/Land Cover Change Statistics From Landsat: A Study of Prime Agricultural Land. *Proceedings of the 14th International Symposium on Remote Sensing of the Environment*, Ann Arbor, MI, pp. 1227-1237

Toll D.L., J.A. Royal, and J.B. Davis (1980). Urban Area Up-Date Procedures Using Landsat Data. *Proceedings of the Fall Technical Meeting of the American Society of Photogrammetry*.

USDA (1992). Forest Statistics for the Northern Piedmont of Virginia. USDA, Forest Service, *Resource Bulletin* SE-127.

USGS (2000). North American Landscape Characterization (NALC) Project/Campaign Document. *Web document*: http://eosims.cr.usgs.gov:5725/CAMPAIGN_DOCS/nalc_proj_camp.html

VDOF (2001). Riparian Forest Buffer Tax Credit: Questions and Answers. *Virginia Forest Landowner Update*, Vol. 15, No. 1. pp. 1.

Vitousek, P.M. (1992). Global environmental change: an introduction. *Annual Review of Plant Ecology and Systematics*, 23, pp. 1-14.

Varlyguin, D., R. Wright, S.J. Goetz, and S.D. Prince (2001). Advances in land cover classification for applications research: a case study from the mid-Atlantic RESAC. *American Society for Photogrammetry and Remote Sensing (ASPRS) Conference Proceedings*. St. Louis, MO, Web document: www.geog.umd.edu/resac

Walsh, M.B. (1979). Landsat Eight Band Two Season Land Cover Classification Compared with Aerial Photographic Interpretation of the Toledo, Ohio Area. *U.S. Army Corps of Engineers, Report No. 139100-1F.*

Weismiller, R.A., S.J. Kristof, D.K. Scholz, P.E. Anuta, and S.A. Momin (1977). Change Detection in Coastal Zone Environments. *Photogrammetric Engineering and Remote Sensing*, 43, pp. 1533-1539.

Wynne, R.H. (2002). Personal communication.

Wynne, R.H. and J.A. Scrivani, (2000). Improving SAFIS forest removal estimates through spectral change detection. *Proceedings of the Second International Conference on Geospatial Information in Agriculture and Forestry*. Orlando, Florida, January 10-12, Vol. 1, pp. 200-207.

Wynne, R.H., R.G. Oderwald, G.A. Reams and J.A. Scrivani, (2000). Optical Remote Sensing for Forest Area Estimation. *Journal of Forestry*, 98, 5, pp. 31 – 36.

Yuan, D., C.D. Elvidge, and R.S. Lunetta (1998). Survey of Multispectral Methods for Land Cover Change Analysis. *Remote Sensing Change Detection: Environmental Monitoring Methods and Applications* (R.S. Lunetta and C.D. Elvidge, editors), Ann Arbor Press, Chelsea, MI, pp. 21- 39

Appendix A

Original Images Used in the Study

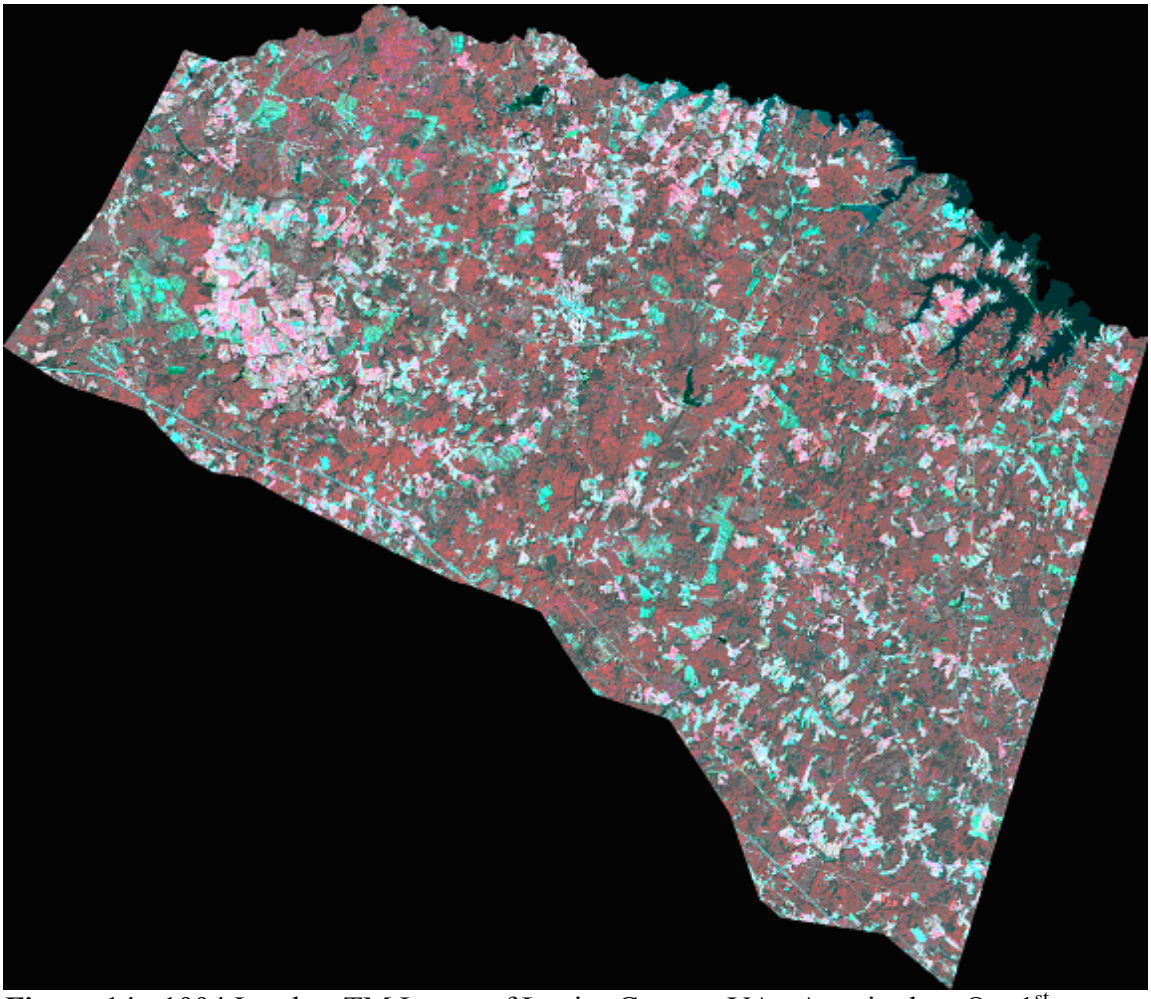

Figure 14 - 1994 Landsat TM Image of Louisa County, VA. Acquired on Oct 1st.

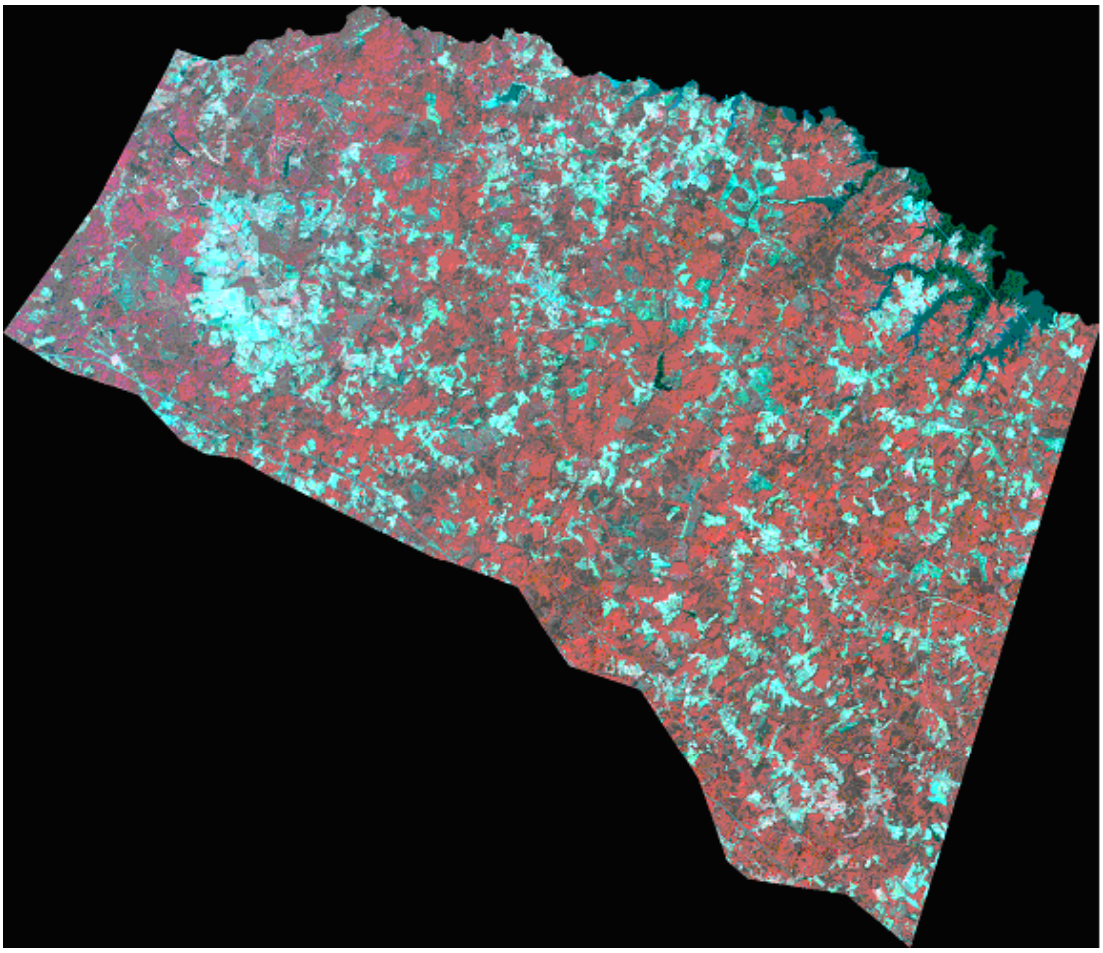

Figure 15 - 1998 Landsat TM Image of Louisa County, VA. Acquired on Sept 26th.

Appendix B

Change Maps Derived from the 8 Techniques Applied to the Original Imagery.

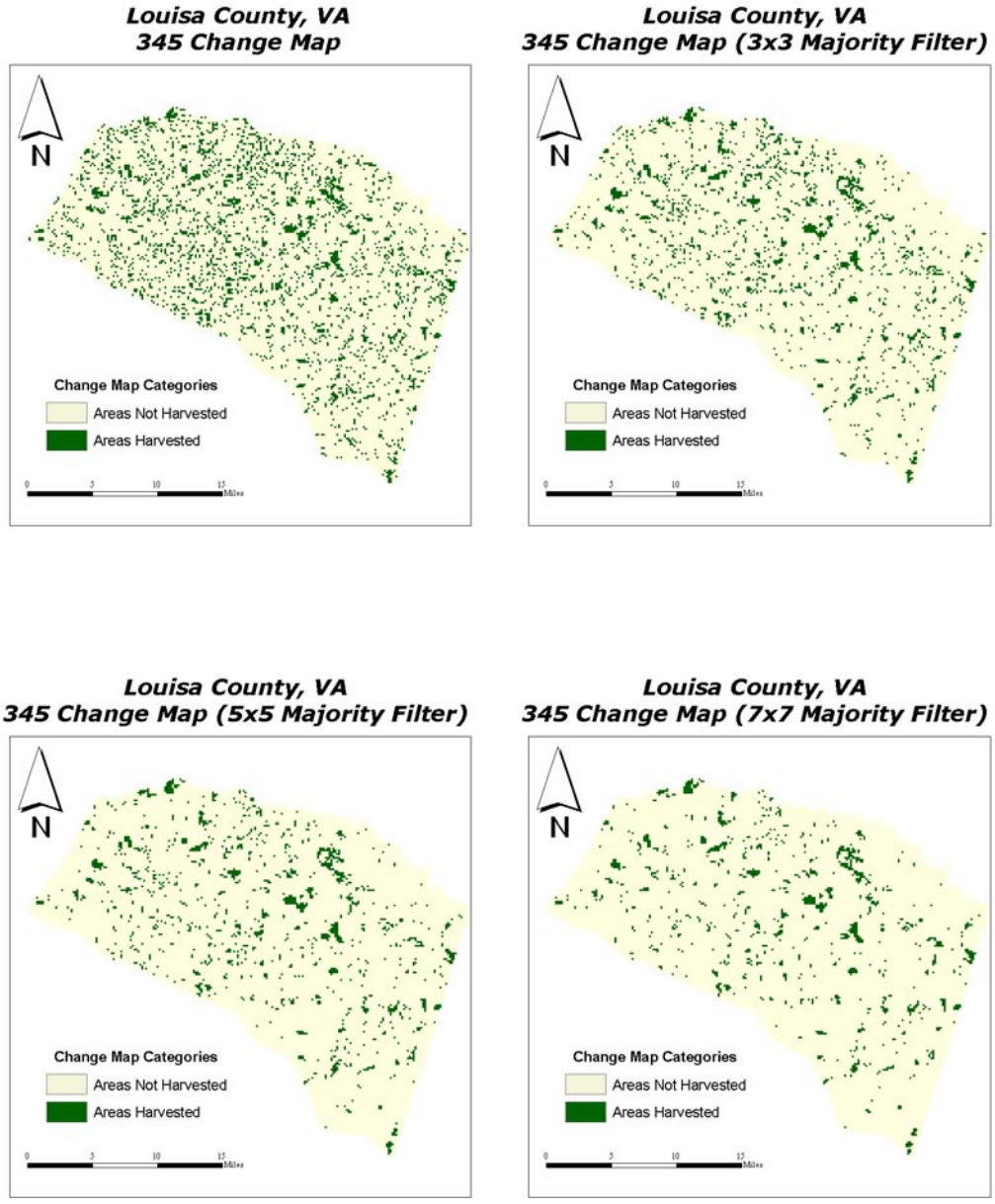

Figure 16 -Change maps derived from the 345 differencing technique.

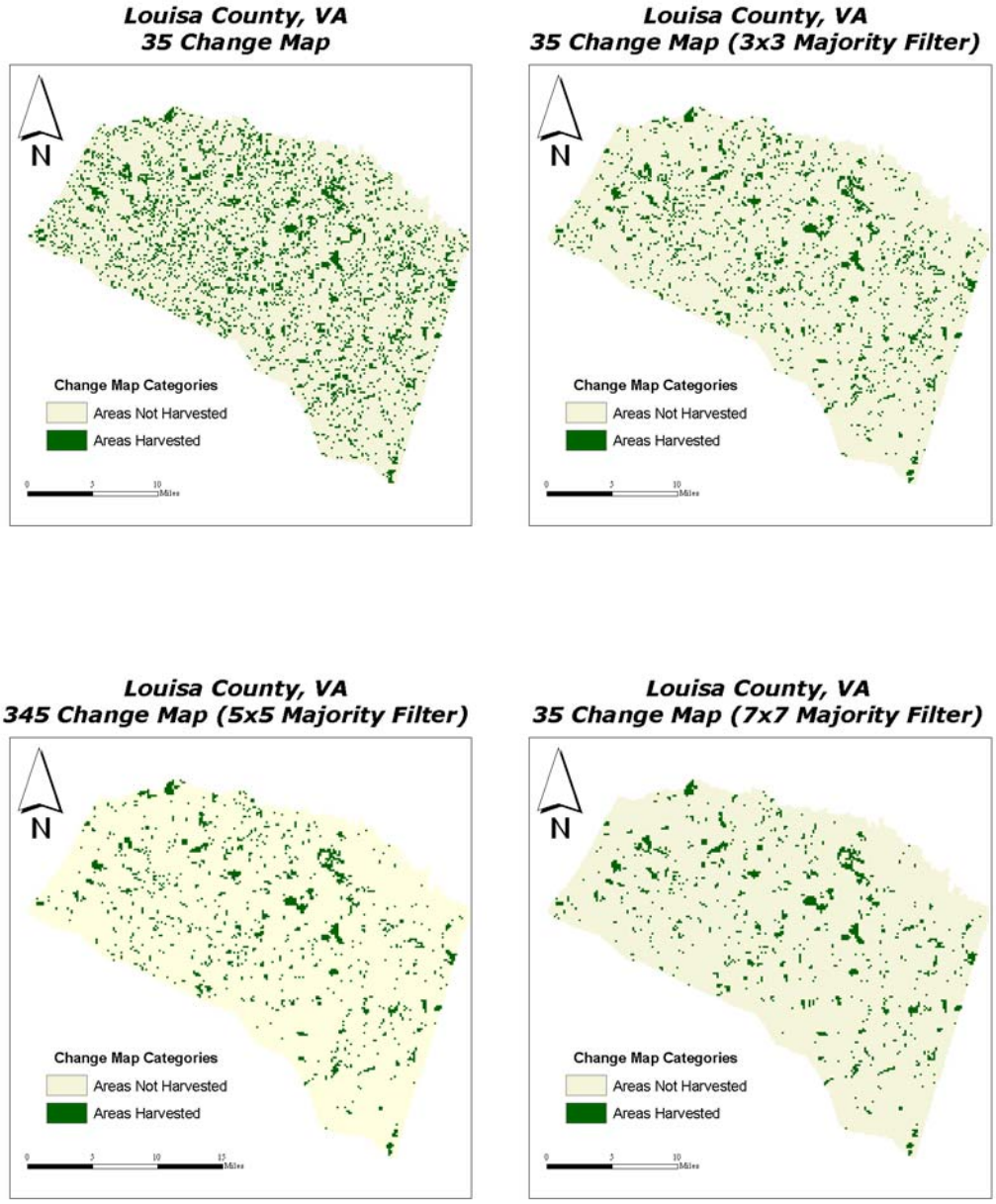

Figure 17 -Change maps derived from the 35 differencing technique.

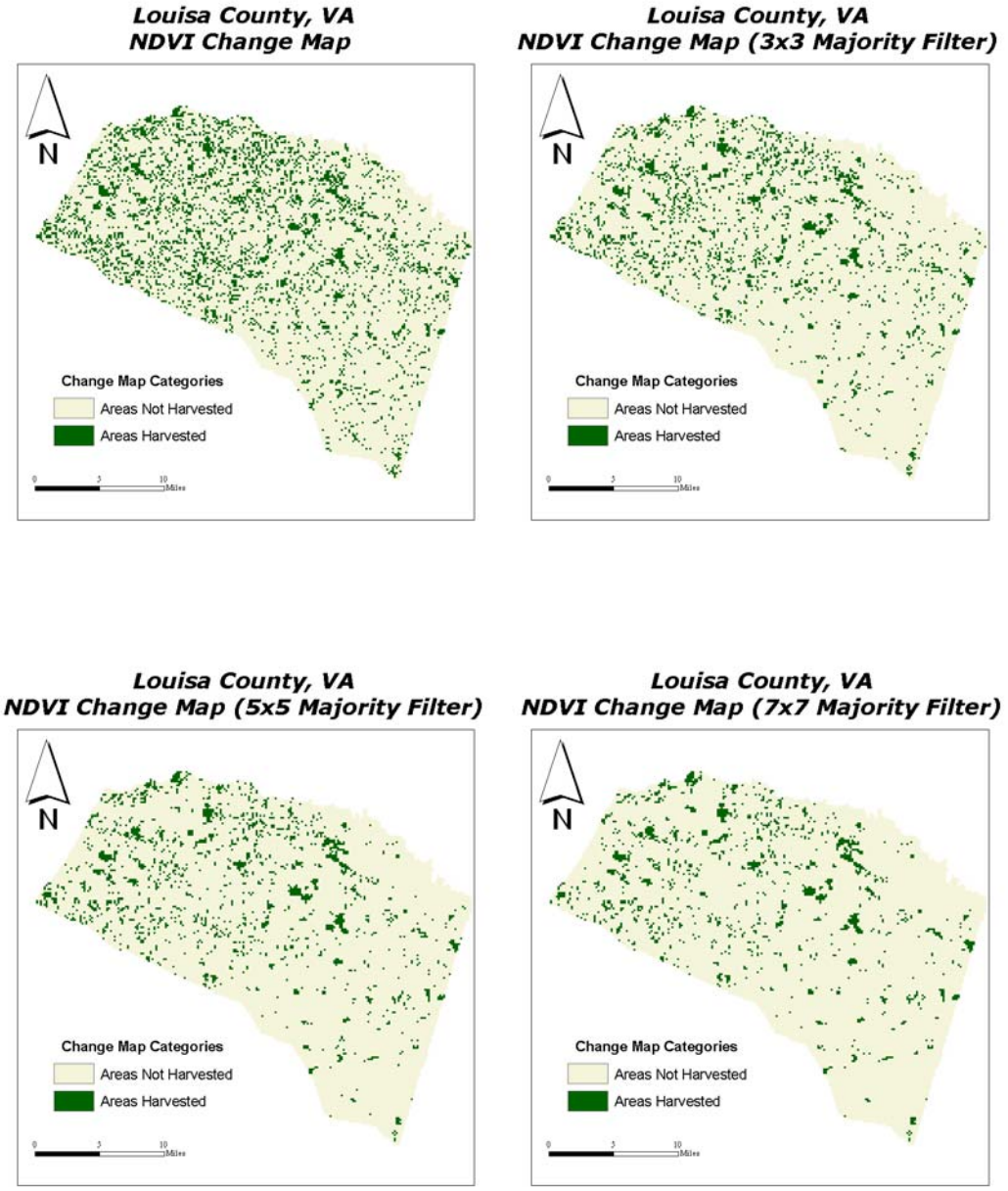

Figure 18 -Change maps derived from the NDVI differencing technique.

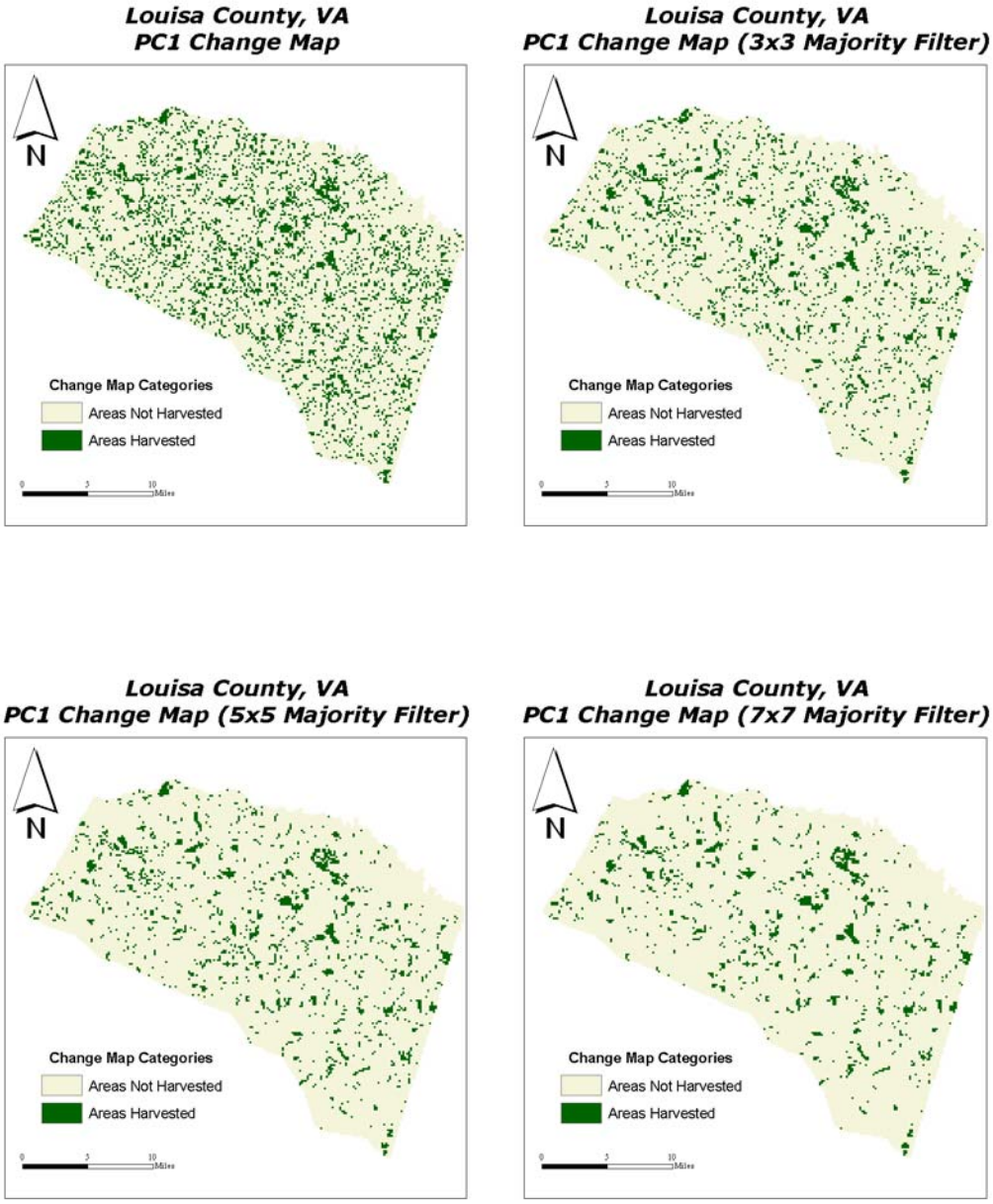

Figure 19 -Change maps derived from the PC1 differencing technique.

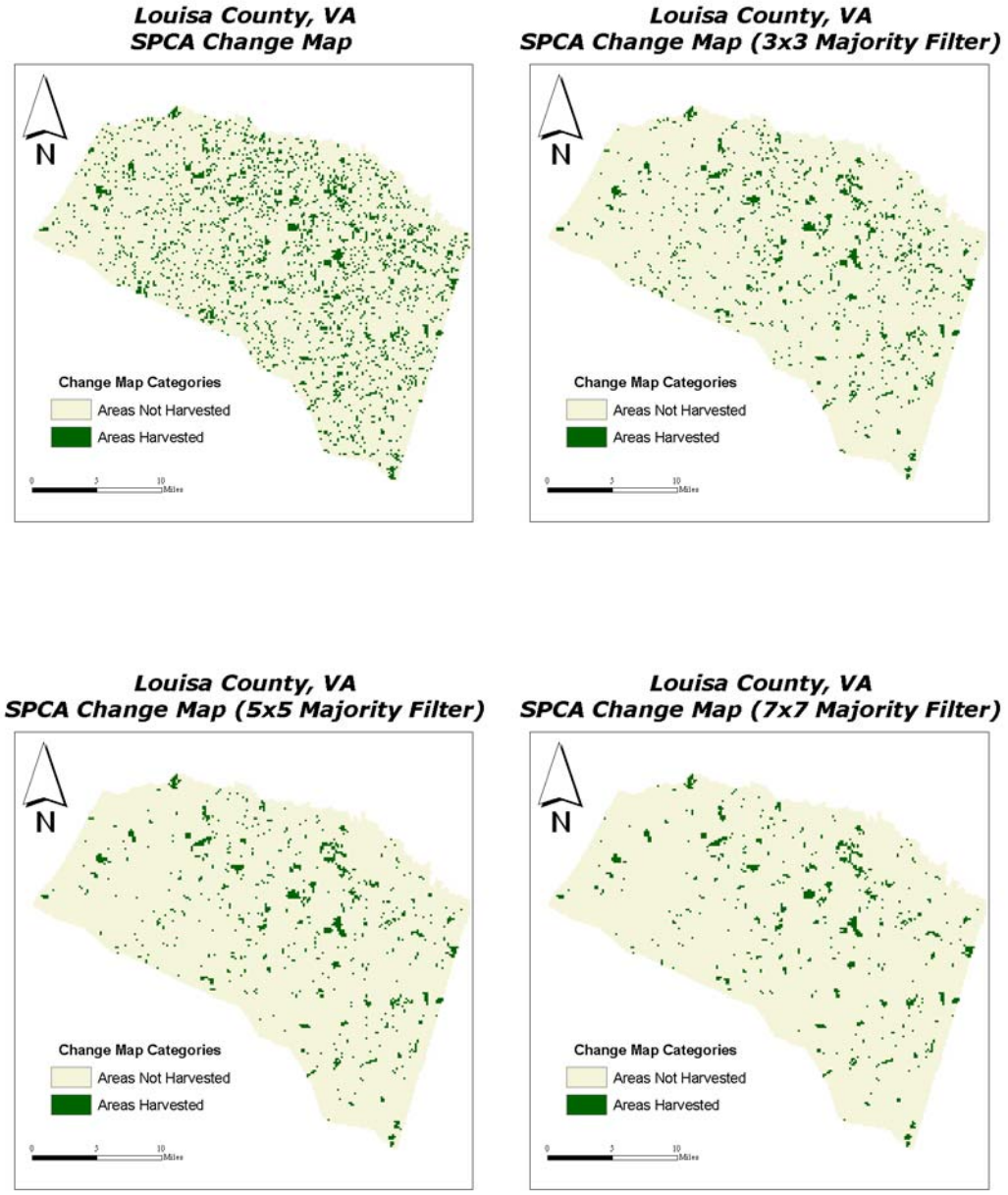

Figure 20 -Change maps derived from the SPCA technique.

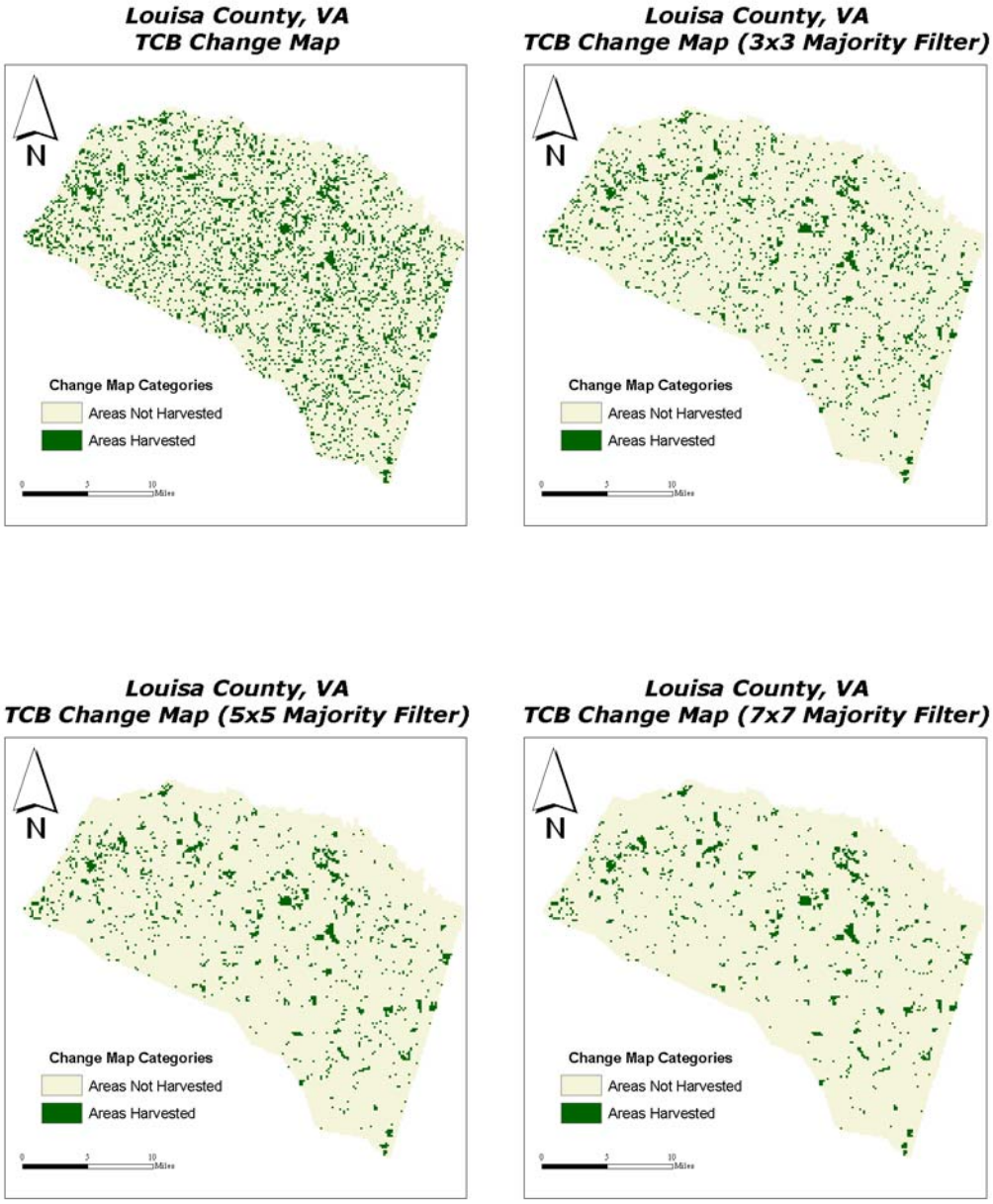

Figure 21 -Change maps derived from the TCB differencing technique.

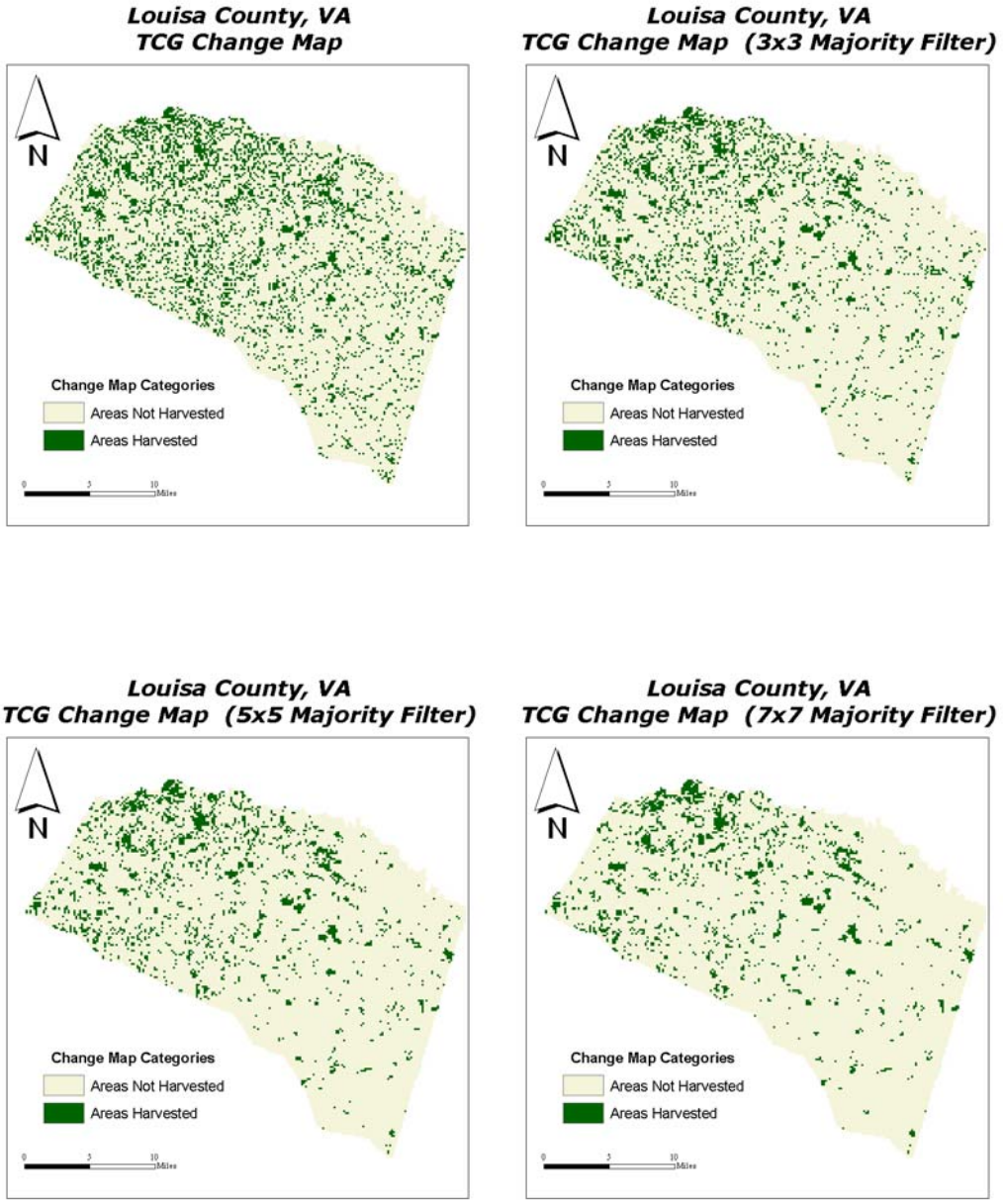

Figure 22 -Change maps derived from the TCG differencing technique.

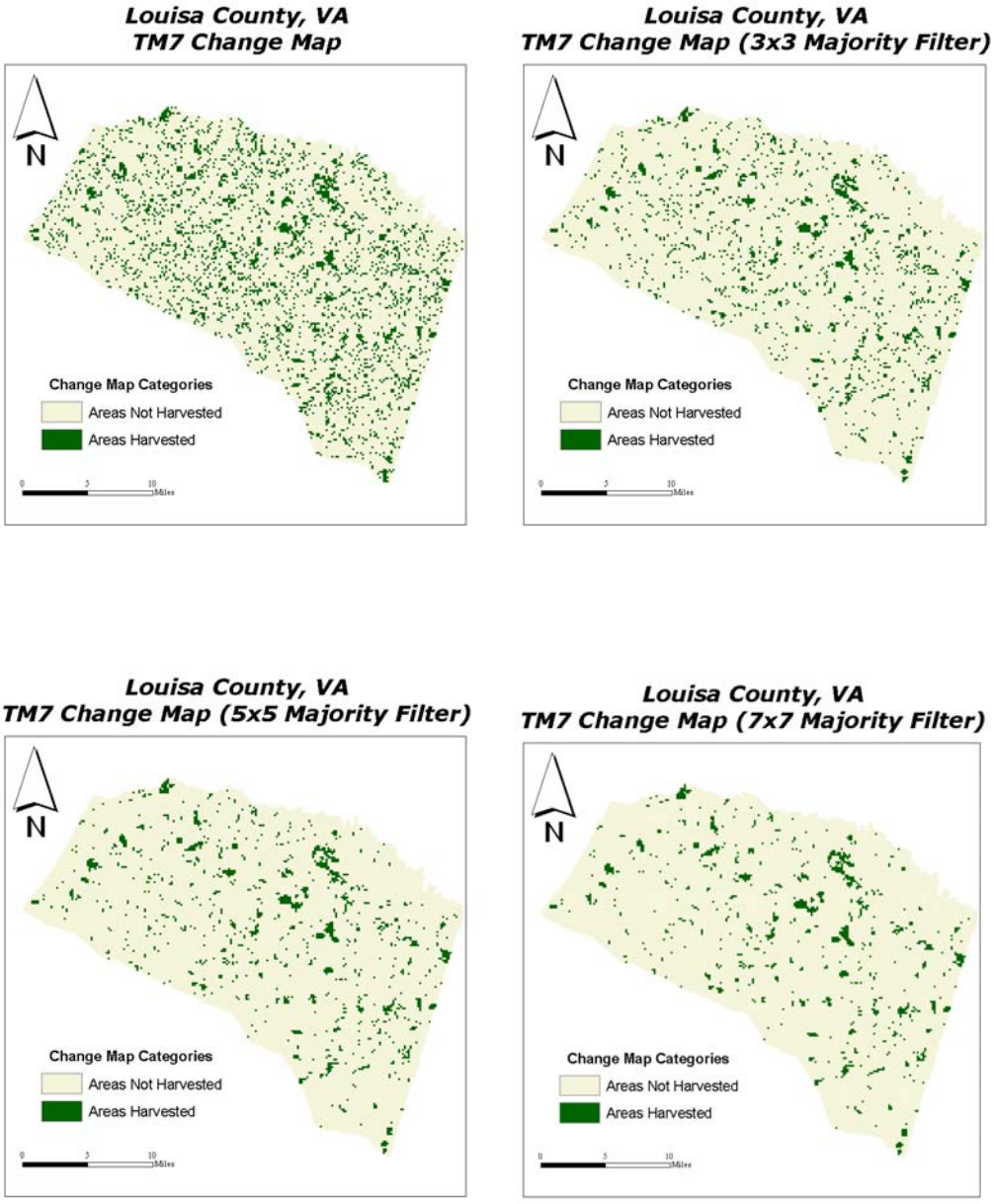

Figure 23 -Change maps derived from the TM7 differencing technique.

Appendix C

Change Models Designed Using Erdas Imagine 8.4.

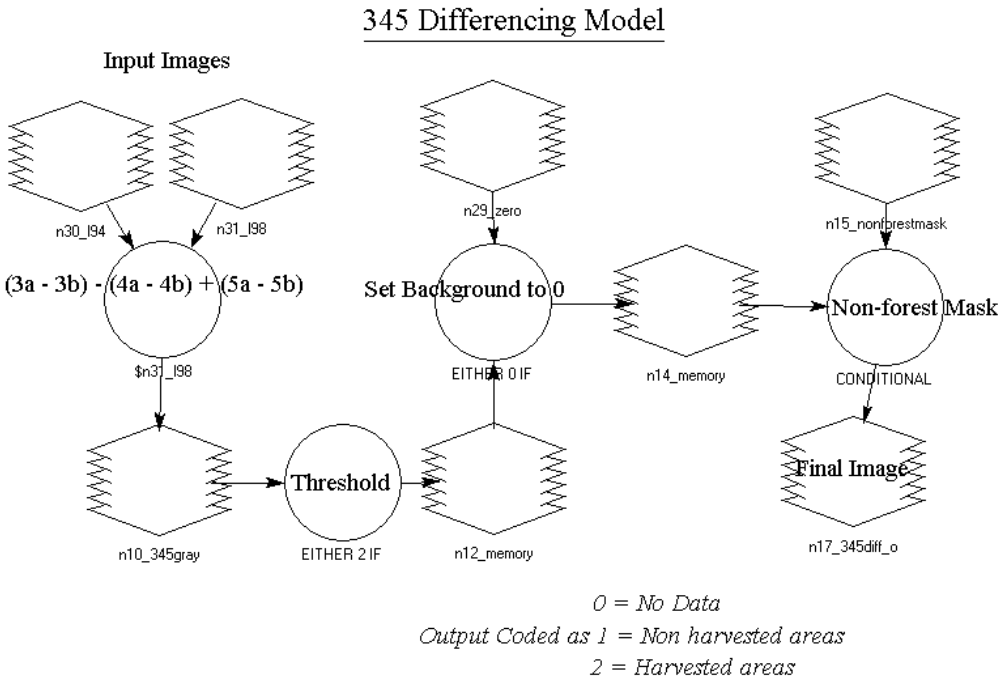

Figure 24 –Model for the 345 differencing technique.

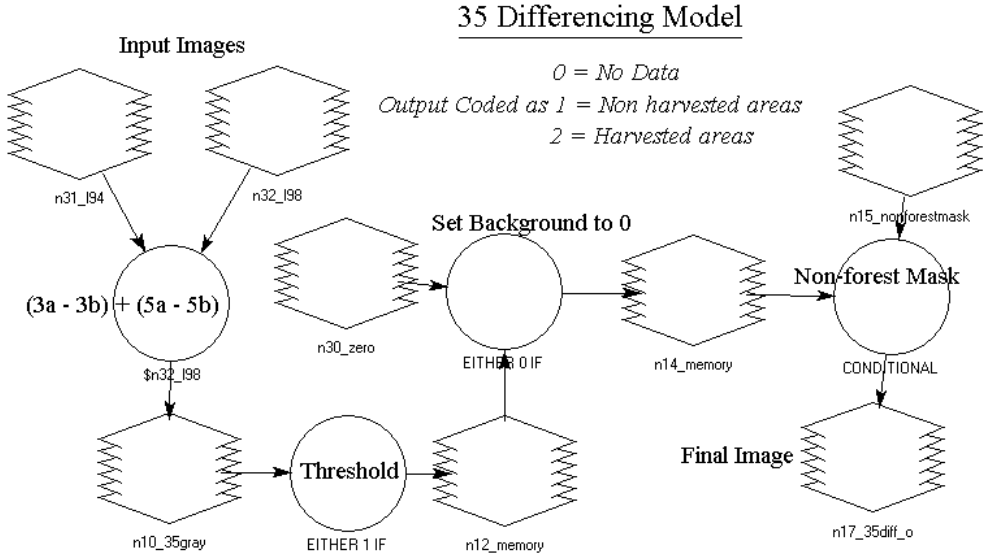

Figure 25 –Model for the 35 differencing technique.

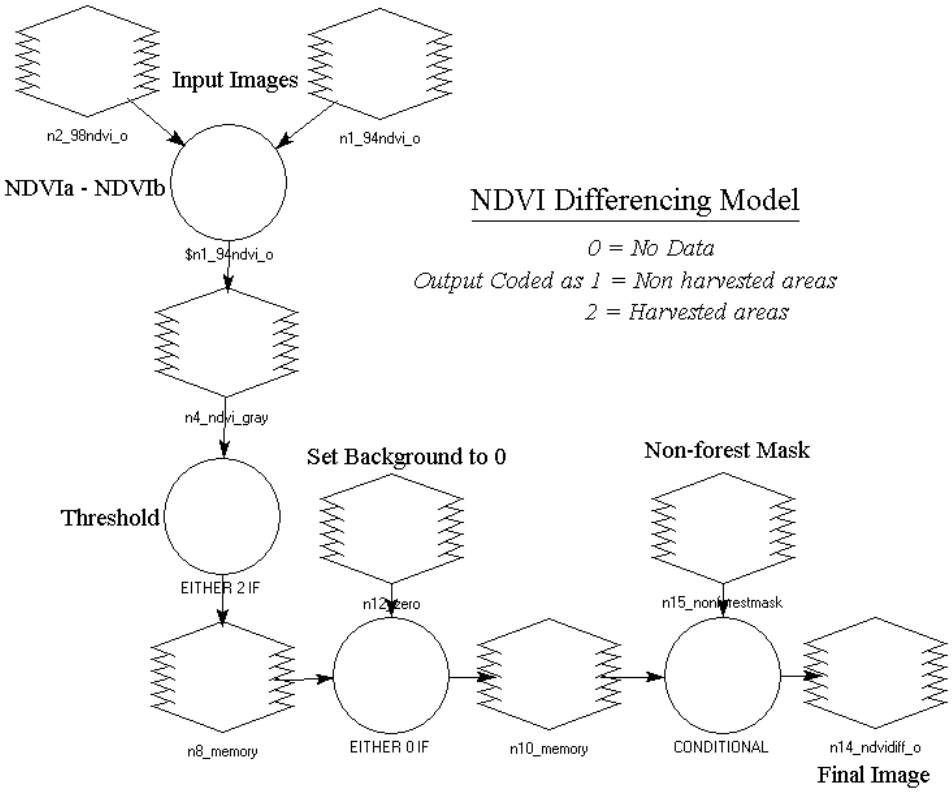

Figure 26 –Model for the NDVI differencing technique.

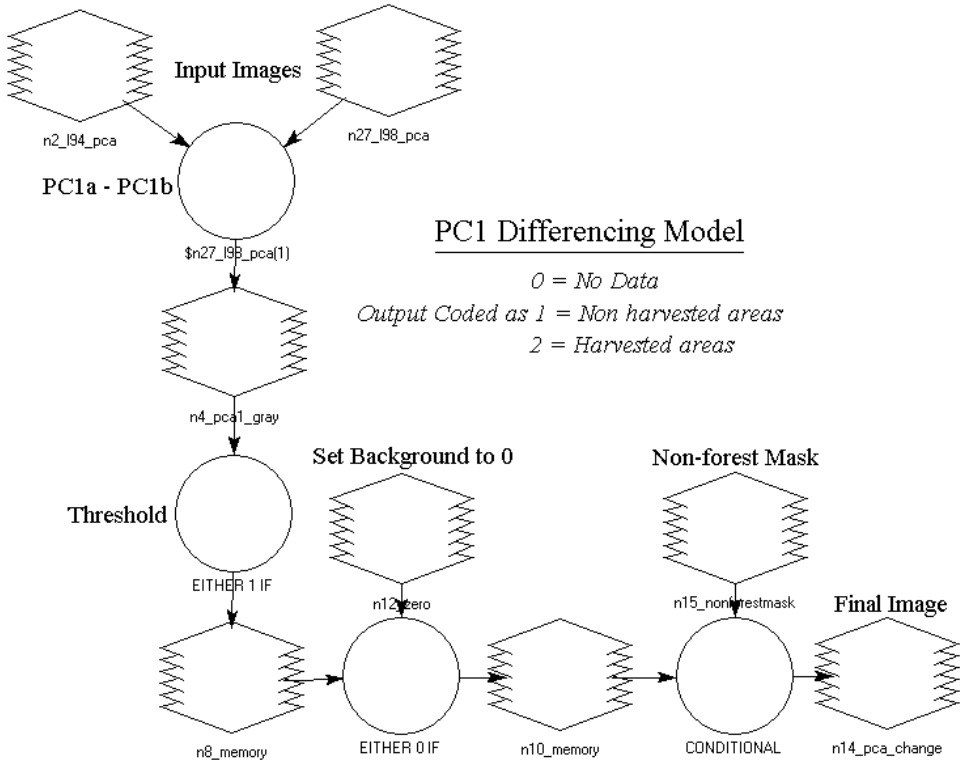

Figure 27 –Model for the PC1 differencing technique.

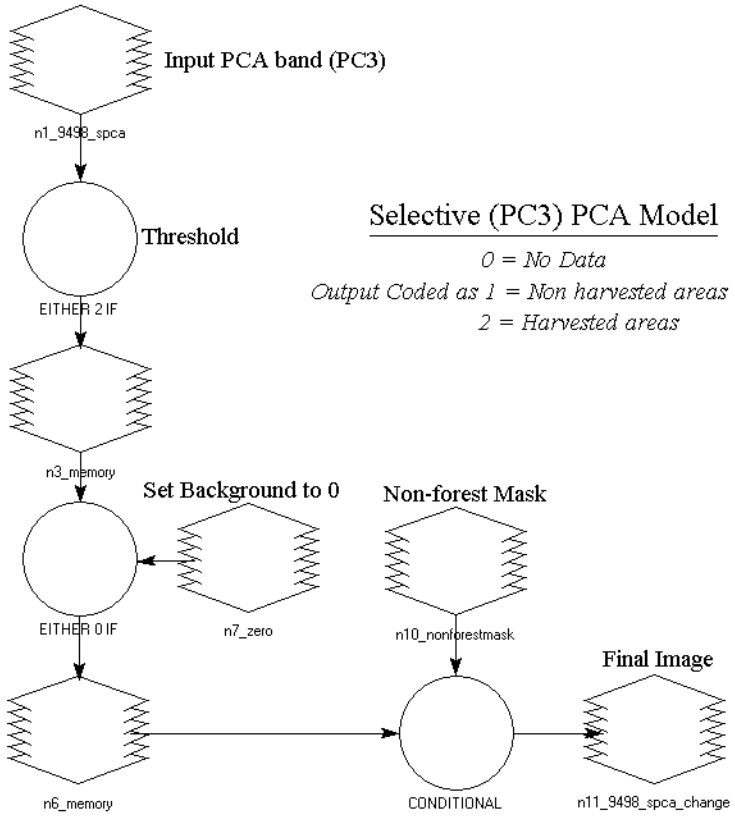

Figure 28 –Model for the SPCA technique.

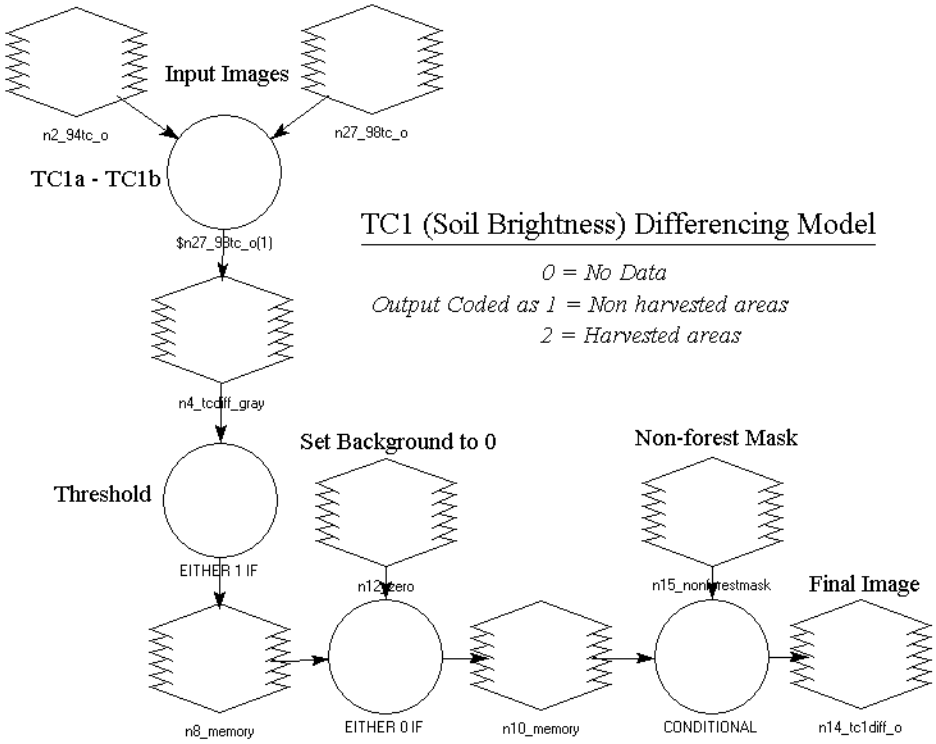

Figure 29 –Model for the TCB differencing technique.

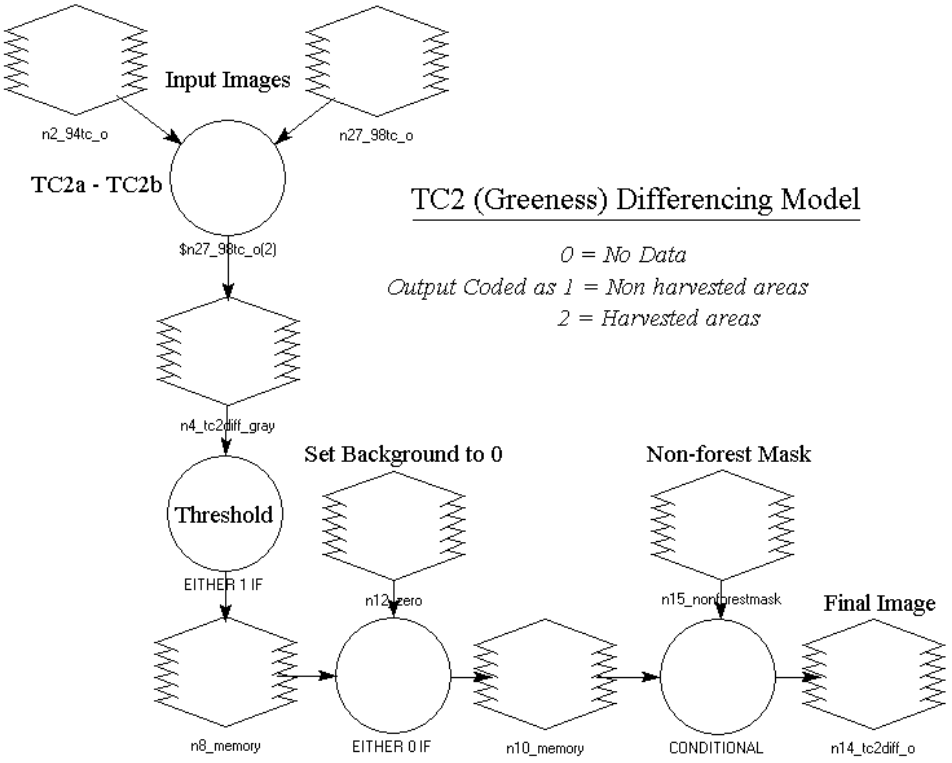

Figure 30 –Model for the TCG differencing technique.

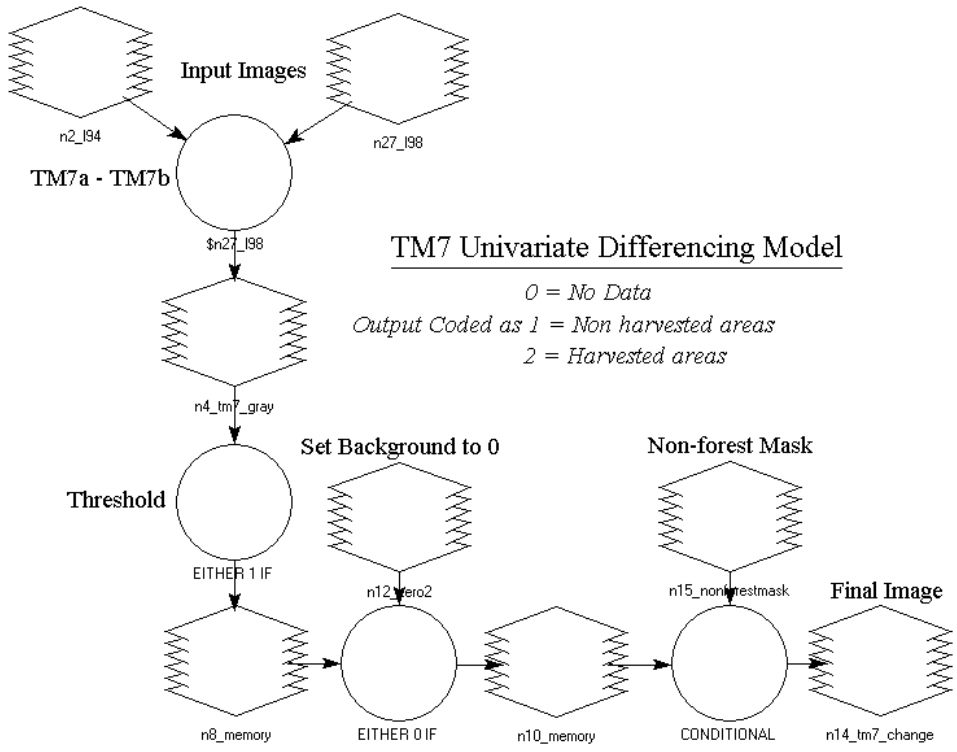

Figure 31 –Model for the TM7 differencing technique.

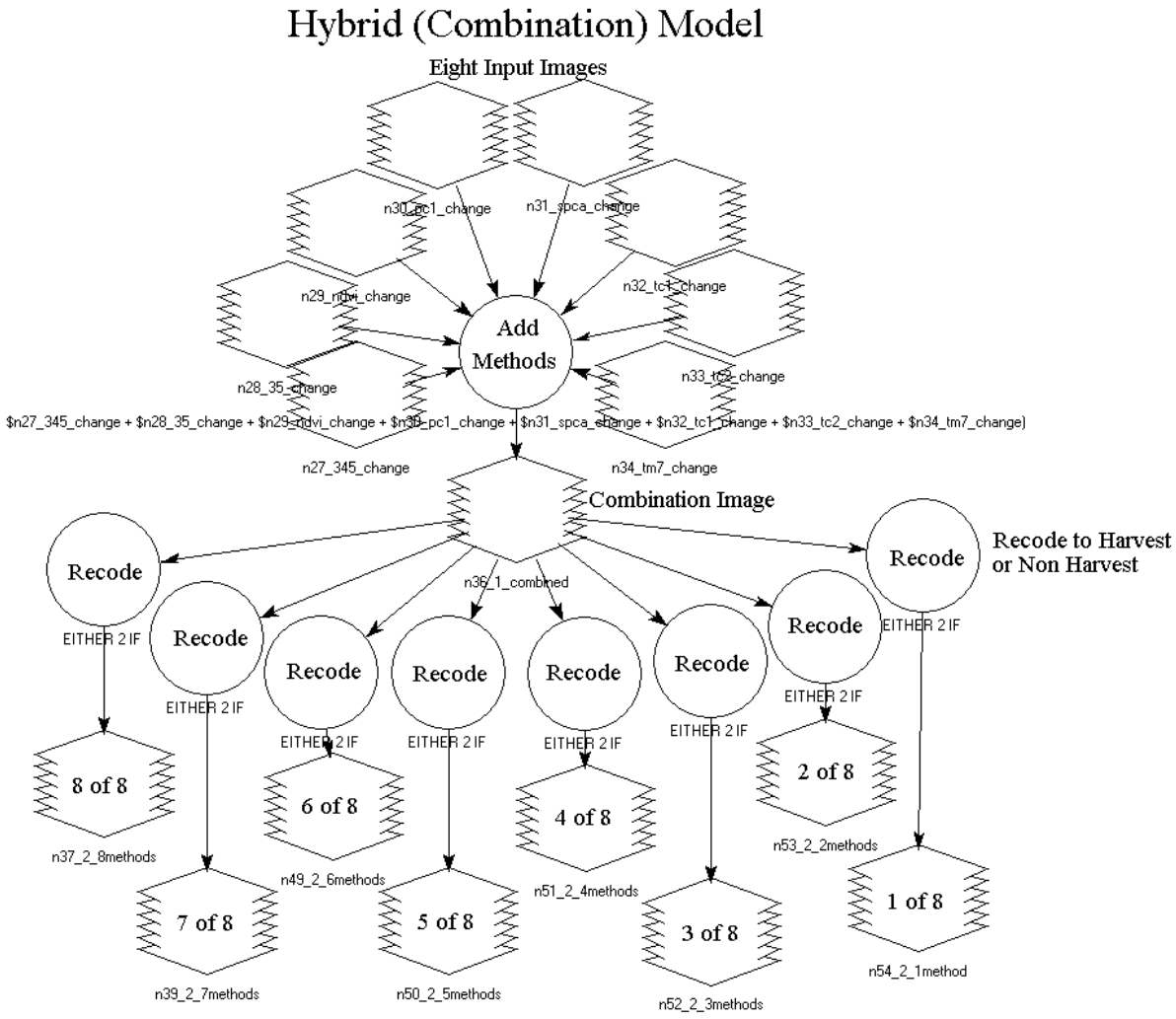

Figure 32 –Model for the Hybrid technique.

VITA

Samuel David Chambers was born on September 12, 1973 in Elizabeth City, NC. In 1991 he joined the United States Marine Corps reserves where he served as an Amphibious Assault Vehicle operator, eventually achieving the rank of Staff Sergeant and the billet of Platoon Sergeant. In 1992 he began attending East Carolina University, and after two years transferred to Elizabeth City State University where he obtained a B.Sc. in Geology with a minor in GIS and Remote Sensing in 1996. While pursuing his undergraduate education, he worked various positions including a summer internship for the Department of Energy in Tupman, CA. After he received his B.Sc., he continued to work at the University as a Laboratories Manager for the Geosciences Department. In addition to maintaining the GIS and environmental research laboratories, he worked on a variety of research grants, commonly in a supervisory role over undergraduate researchers.

In the fall of 2000, he entered the Master's program in the Department of Geography at Virginia Tech, concentrating in GIS and Remote Sensing. He obtained a M.S. in July 2002. He recently accepted a position as a Geographer for the Joint Warfare Analysis Center in Dahlgren, VA.